THE
PHYSICAL REVIEW
A Journal of Experimental and Theoretical Physics
VOL. 44, No. 6 SEPTEMBER 15, 1933 SECOND SERIES

The Evaporation of Atoms, Ions and Electrons from Caesium Films on Tungsten

JOHN BRADSHAW TAYLOR AND IRVING LANGMUIR, *Research Laboratory, General Electric Company*
(Received January 19, 1933)

Precision methods for measuring the number of caesium atoms adsorbed on tungsten are described. With these methods for determining θ (the fraction of the tungsten surface covered with Cs), the rates of atom, ion and electron emission are measured as functions of θ and T, the filament temperature. *The rate of atom evaporation*, ν_a, increases rapidly with θ and with T. At low filament temperatures and high pressures of Cs vapor the concentration of adsorbed Cs atoms approaches a limit 3.563×10^{14} atoms cm^{-2} of true filament surface (one Cs atom for four tungsten atoms). This film ($\theta=1$) exhibits all the characteristics of a true monatomic layer. The formation of a second layer begins only at filament temperatures corresponding to nearly saturated Cs vapor. A theory of the formation of a second and of polyatomic layers is given and experiments supporting it are described. *The heat of evaporation* (given by the Clapeyron equation) for Cs atoms from clean tungsten is 2.83 volts (65,140 calories), 1.93 volts or 44,473 calories at $\theta=0.67$, and 1.77 volts or 40,757 calories at $\theta\backsimeq1$. The adsorbing tungsten surface after proper aging is homogeneous, except that about 0.5 percent of it (active spots) can hold Cs more firmly than the rest. The procedure in obtaining *electron* (ν_e) and *ion* (ν_p) *emission* for zero field and the large changes in the effect of external field with θ are described. From both ν_e and ν_p the contact potential V_c is calculated, agreeing, except for very concentrated films, with V_c calculated entirely from data on neutral atom evaporation. At constant temperature the electron emission increases to a maximum at $\theta=0.67$ and decreases as $\theta=1$ is approached. The positive ion emission increases rapidly to a maximum at $\theta\backsimeq0.01$ and then decreases. The work function (exponent in Dushman type equation) for electrons at $\theta=0.67$ is 1.70 volts (clean tungsten = 4.62 volts). The work function for ions is 1.91 volts at $\theta=0$, and 3.93 volts at $\theta=0.67$. It is shown by experiment that the saturated ion current from a clean hot (1200–1500°K) tungsten filament is an accurate measure (experimental error of about 0.2 percent) of the number of atoms striking the filament per second. *The condensation coefficient* (α) for atoms striking a tungsten filament is proved by experiment to be unity from $\theta=0$ to nearly 1. The important bearing of this fact and of the experimentally observed existence of *surface migration* or diffusion on the *mechanism of evaporation and condensation* in dilute and concentrated films is discussed. In addition surface migration is correlated with irregular ion evaporation rates occurring when two phases (dilute and concentrated films of Cs) exist on the tungsten surface. *Transient effects* in which θ changes with time are studied and entirely explained by the observed rates of evaporation and condensation. This and other facts are used to justify a *surface phase postulate* according to which all the properties of the adsorbed film are uniquely determined by θ and T.

I. INTRODUCTION

CAESIUM films on tungsten form an important and interesting case of adsorption. The adsorbed atoms are held on the tungsten by such large forces that remarkable changes in the thermionic properties of the tungsten can be observed. As the tungsten surface can be completely cleaned and the supply of caesium atoms can be controlled, this system is capable of furnishing quantitative information regarding adsorption and the electrical properties of surface films.

Films of alkali metal atoms on tungsten have been the subject of several investigations. Langmuir and Kingdon[1] found that caesium

[1] I. Langmuir and K. H. Kingdon, Science **57**, 58 (1923); Proc. Roy. Soc. **A107**, 61 (1925).

atoms adsorbed on tungsten greatly increased the electron emission of the tungsten and showed that caesium atoms striking a hot clean tungsten filament were converted into positive ions which could be collected by a plate at a negative potential. Both the electron and ion emissions were functions of the temperature (T) of the filament and of the fraction (θ) of the surface covered with caesium. The electron emission increased to a maximum at a certain value of θ and decreased with further increase in θ. The positive ion emission became appreciable only for low values of θ; at higher values of θ, caesium films evaporated only as neutral atoms. Only rough estimates of θ were made in this work.

Recently Langmuir[2] has treated the properties of caesium adsorbed on tungsten in a general discussion of evaporation, condensation, and adsorption, and has given a partial derivation of equations used in this paper.

Becker[3] has studied the evaporation of atoms, ions, and electrons from caesium films on tungsten and made measurements of θ. He attributed the maximum electron emission to a single complete layer of caesium atoms and the subsequent decrease in emission to the formation of a second layer of caesium atoms.

The present investigation was undertaken for the purpose of determining quantitatively the dependence of the rates of neutral atom evaporation (ν_a), ion emission (ν_p), and electron emission (ν_e) on θ, filament temperature T, and the field strength; ν_a, ν_p and ν_e represent the number of atoms, ions, or electrons evaporating per unit area, per unit time. To facilitate correlation of ν_p and ν_e with θ, the greater part of the work has consisted in establishing θ as a function of caesium pressure and filament temperature.

In the steady state,

$$\alpha\mu_a = \nu_a; \tag{1}$$

that is, the number of atoms evaporating per unit area per unit time (ν_a) is equal to the number condensing, which is equal to the number arriving per unit area per unit time (μ_a), multiplied by the condensation coefficient α. Evidence regarding the nature of α will be given (Section XI) and it will be shown that under our experimental conditions α is equal to unity. Therefore the experiments which give θ as a function of μ_a also give ν_a as a function of θ.

Let us now postulate that ν_a, ν_p and ν_e are functions of θ and T only. The distribution of atoms is assumed to be uniform and independent of the way (e.g., by evaporation or condensation) in which θ was reached. This "surface phase postulate" will be discussed and justified in Section XI. Determinations of ν_e and ν_p at various pressures then enable us to express ν_e and ν_p as functions of θ and T.

II. Apparent and True Filament Surface and Definition of θ

The apparent area S_A of the filament surface is that calculated from the dimensions of the filament (πld). Actually after heating to 2900° during aging, a tungsten filament becomes etched and develops[4] dodecahedral crystal faces (110) in which there are 1.425×10^{15} tungsten atoms per cm^2. The actual surface area S is thus greater than S_A (see Fig. 1).

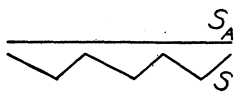

Fig. 1. True (S) and apparent (S_A) filament surface.

It so happens that crystals of metallic caesium[5] have the same type of lattice (body-centered cubic) as tungsten and the lattice constant (6.17A) is almost exactly double that of tungsten (3.15A). Thus if, in a complete monatomic film of caesium on tungsten, the caesium atoms arrange themselves in a surface lattice identical with that of the tungsten surface but with double spacing, there will be one caesium atom for every four tungsten atoms, all the adatoms will be similarly placed with respect to the underlying tungsten atoms, and the adatoms will be at the same distances from one another as in metallic caesium.

Because the strong forces between the caesium

[2] I. Langmuir, J. Am. Chem. Soc. **54**, 2798 (1932).

[3] J. A. Becker, Phys. Rev. **28**, 341 (1926); J. Am. Electrochem. Soc. **55**, 153 (1929).

[4] I. Langmuir, Phys. Rev. **22**, 374 (1923).

[5] Simon and Vohsen, Zeits. f. physik. Chemie **133**, 165 (1928).

and the tungsten atoms must tend to make the adatoms occupy definite elementary spaces[6] determined by the tungsten lattice, we believe we are justified in adopting this 4 to 1 relation as a postulate in our further investigations. We may therefore put for the true surface concentration σ_1 of a complete caesium film on tungsten

$$\sigma_1 = 3.563 \times 10^{14} \text{ atoms cm}^{-2}. \quad (2)$$

Experiments which will be described in Section V and XII have shown that with the particular filament used, the apparent surface concentration σ_{A1} for a complete film of caesium on tungsten is

$$\sigma_{A1} = 4.80 \times 10^{14} \text{ atoms cm}^{-2}. \quad (3)$$

The ratio σ_{A1}/σ_1, which is 1.347, is thus equal to S/S_A, the ratio of the true to the apparent filament surface. Tonks has calculated[7] that with a random distribution of dodecahedral crystals the *minimum value* of S/S_A is 1.225, a value which supports our postulate.

We intend to test this postulate in future work by comparing values of σ_{A1} obtained with adsorbed films of caesium, rubidium and potassium on a single tungsten surface. If the value σ_1 as given above is correct, we should expect that σ_{A1} will be the same for all alkali metals.

Let σ_A be the apparent surface concentration of adatoms obtained by dividing the total number of adatoms by S_A, the apparent surface area (πld). Then the true surface concentration σ is $\sigma_A S_A/S$. It is probable that S/S_A may vary somewhat for different filaments according to the aging treatment and the fineness and orientation of the crystals. The intrinsic properties of the adsorbed film are presumably dependent on σ rather than σ_A. Since, however, our knowledge of σ depends upon our postulated value of σ_1, as given by Eq. (2), it is preferable to express these properties as functions of the covering fraction θ defined by

$$\theta = \sigma_A/\sigma_{A1}. \quad (4)$$

All the values of θ in this paper have been calculated in this way from σ_A by using the value of σ_{A1} given by Eq. (3). It should be noted that θ is also equal to σ/σ_1.

We must also have clearly in mind the relation of S and S_A to our definitions of μ and ν. We shall define μ_a as the number of incident atoms per unit time per unit area of *apparent surface* S_A. Thus from the kinetic theory

$$\mu_a = p(2\pi mkT)^{-\frac{1}{2}} = 3.796 pT^{-\frac{1}{2}} \text{ atoms cm}^{-2} \text{ sec.}^{-1} \quad (5)$$

where p is the pressure in baryes and T is the temperature of the caesium vapor.

In a similar way we define ν_a as the number of atoms which escape from the filament by evaporation per unit time per unit area of *apparent surface* (S_A).

We wish, however, to know the rate of evaporation per unit area of true surface S for this alone should be an intrinsic property of the adsorbed film.

In the steady state to which Eq. (1) applies, the condensation on and evaporation from each element of area must balance. The atomic flux density in the neighborhood of the filament must therefore be isotropic just as is the heat radiation within an enclosure at uniform temperature. The values of μ and ν over the surface of S, in Fig. 1, must thus be the same as over the surface S_A.

Consider now the irreversible evaporation of adatoms from a filament in a space in which $\mu = 0$. We see from S in Fig. 1 that a large fraction of the atoms that evaporate from the valleys (and a smaller fraction from the peaks) are intercepted by the surface of the opposing peaks before they can escape. The concentration of adatoms thus decreases near the peaks faster than in the valleys unless surface mobility equalizes their concentration.

If mobility does maintain a uniform θ and if $\alpha = 1$ so that all incident atoms condense, it follows from the reversibility principle (see Section XII) that the emission occurs in accord with Lambert's cosine law. The situation is exactly analogous to that in optics where the brightness of an incandescent black body is independent of its contour.

During irreversible condensation from a vapor with a given μ, the concentration at the peaks

[6] I. Langmuir, J. Am. Chem. Soc. **38**, 2287 (1916); **40**, 1366 (1918).

[7] L. Tonks, Phys. Rev. **38**, 1030 (1931).

should increase faster than in the valleys, assuming no mobility. Since the experiments (see Section XI) have shown no difference in properties of a film with a given average value of θ whether it was obtained by irreversible condensation or evaporation, we must conclude that surface mobility equalized θ over the surface. Because of this mobility and the fact that $\alpha=1$, we may therefore conclude that the values of ν defined in terms of apparent surface are identical with the evaporation rates per unit area of true surface.

III. Methods for Determining θ

There are four methods available for determining θ. Common to all methods is the measurement of the caesium vapor pressure (controlled by bulb temperature) in terms of μ_a, by observing the positive ion current to a collector at a negative potential with respect to a hot (>1200°K) tungsten filament. As will be demonstrated later, every atom striking the filament leaves as a positive ion so that I_p/e, the saturation positive ion current density divided by the electronic charge, gives μ_a.

Becker's method

Becker observed the time (t_m) required for the electron emission from a filament (initially cleaned by flashing) to reach a maximum value while the filament at temperature T_1 was being coated by a constant supply of Cs vapor. At the maximum, θ was assumed to be unity, that is, the film was taken to be a complete monatomic layer. It was then possible to raise the temperature of the filament to various temperatures (T_2), where the equilibrium θ was less than unity. If the temperature was now lowered to T_1, the electron emission again passed through a maximum as θ increased through unity. The time (t_3) needed for this completion of the film served to measure the θ at T_2 since $\theta=1-t_3/t_m$.

Direct flashing method

If a tungsten filament having a film for which θ is less than 0.08 is suddenly flashed in an accelerating field at a high temperature, all the caesium evaporates as ions giving a ballistic kick on a galvanometer. The filament area together with the ballistic calibration of the galvanometer allow calculation of σ_A and hence of θ.

Two filament method

As shown diagrammatically in Fig. 2, two parallel straight tungsten filaments, A and B, were mounted near the axis of three coaxial

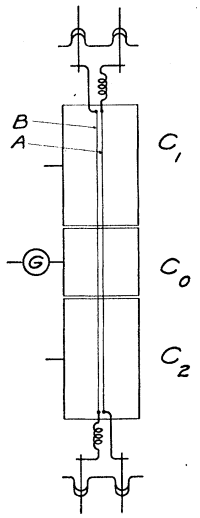

FIG. 2. Filament and collector arrangement in two filament method (diagrammatic).

cylindrical electrodes c_1, c_0 and c_2, placed end to end so that by the guard-ring principle the electron or ion emissions from a known length of the central part of either filament could be measured. The tube is highly evacuated but contains saturated caesium vapor whose pressure is controlled by the tube temperature. The rate of arrival of atoms, μ_a, is measured with B at a temperature of ~1200°K. This steady current is then balanced out so that only changes in current are indicated by the galvanometer (G) connected to c_0; c_1, c_2 and c_0 were usually maintained at 45 volts negative to filament B. The potential of filament A is made 41 ± 2 volts negative to B (4 ± 2 volts positive to c_1, c_2 and c_0). Filament A is then cleaned by flashing at 2400°K. After a steady state (θ) is reached on its surface at any of a series of lower temperatures (300–1200°K), the temperature of A is suddenly raised to about 1800° so that at these voltages all the adsorbed atoms evaporate instantly as neutral atoms, which travel in straight

lines towards the cylinders c. A definite fraction f of these, however, are intercepted by the hot filament B and are converted into ions which pass to the cylinder c_0. The resulting ballistic kick indicated by the galvanometer, together with the known diameters of A and B and the distance of A from B give data for the calculation of σ_A and θ.

The use of the second filament B as a means of measuring concentrations on filament A too high to be flashed directly from A as ions was suggested by Dr. Tonks of this laboratory.

The potential chosen for filament A insures that neither ions nor electrons shall pass to c_0 as the adsorbed atoms are suddenly evaporated. The correct potential for A is most easily found by flashing A when nearly fully coated, with B cold. If A has been made too negative with respect to c_0, a ballistic kick due to electrons is observed; if not sufficiently negative a kick due to ions is noted. With the correct adjustment (critical only to about ± 2 volts) there is no detectable galvanometer deflection when A is flashed even if the initial values of θ on A are varied from 0 to above 1. This fact that the potential of A can be varied as much as 4 volts without detectable galvanometer deflections when B is cold proves that the zero value of current is not due to a balance between electron and ion currents from A, but that each of these currents is zero. This is undoubtedly caused by space charge limitation of the currents during the excessively short time that they can flow while the filament is being flashed. We therefore believe that no source of error is introduced into these measurements by currents from A. Although the sudden evaporation of atoms was usually accomplished by heating the filament by a condenser discharge, increasing the filament current to a value giving a temperature of about 1800° by closing a switch in a battery circuit also gives sufficiently rapid evaporation.

The accumulation method

If μ_a is small, changes in the properties of the film with time can be measured as θ increases slowly from zero. In this method ν_a must remain equal to zero since σ_A and θ are found from the product $\mu_a \times t$. This is accomplished either by working in the lower ranges of θ or at low filament temperatures.

Comparison of the methods for determining θ

(a) Becker's method may be used to determine θ's from about 0.01 to the optimum value θ_{opt} which gives the maximum in the electron emission; it will be shown later that $\theta_{opt}=0.67$. The method requires not only that θ_{opt} shall be attained and that the electron emission at the optimum be measurable, but also that re-evaporation of atoms is negligible until the maximum is passed. Thus with the sensitive galvanometer used in the present experiments (7×10^{-11} amp./mm) the allowable μ_a was limited to the range between approximately 6×10^{11} and 2×10^{13}, using a testing temperature (T_1) of $\sim$550°K. At lower testing temperatures the electron emission cannot be measured. A higher testing temperature raises the lower limit for μ_a. Even though θ_{opt} may be passed through, unless the testing temperature is low enough, atom evaporation may begin near θ_{opt} causing an increase in the time (t_3) required to reach θ_{opt} and a consequent error in the determination of θ. At higher values of μ_a the coating time becomes too short in comparison with the times required to bring the filament from a high temperature to a steady state at the lower testing temperature. For example, a 2 mil filament requires $\sim$15 seconds to cool from 1220°K to 600°K. A filament in a bulb containing caesium at room temperature is completely coated in less than one second. The method also fails at high pressures because the θ's to be measured may already be above the optimum.

We have often found another serious difficulty in the application of Becker's method. Fig. 3 shows emission *vs.* time curves taken as in Becker's method. The curve a with a single maximum is obtained for caesium on a clean homogeneous tungsten surface. With extremely minute traces of gaseous impurities which are sometimes hard to avoid but which do not interfere with the application of the other methods of determining θ, we have often obtained two maxima as shown in curve b. With slight modification of the conditions the two maxima may merge into one. In such cases

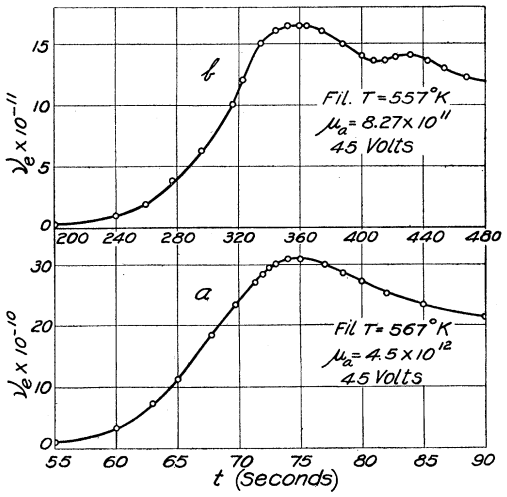

FIG. 3. Electron emission *vs.* time curves as obtained in Becker's method for measuring θ. (a) Clean filament, (b) partly gas covered.

difficulties of interpreting the curves may lead to considerable error in the determination of θ.

(b) The direct flashing method is applied only below $\theta \sim 0.08$ but is so extremely sensitive that θ as low as 10^{-4} can be measured easily.

(c) The accumulation method may be used to produce any value of θ provided μ_a is kept below $\sim 10^{13}$ to give sufficient time for observations. It should find a useful application in the study of contact potentials. Known changes in the surface condition of an electrode receiving electrons can be produced. The resultant changes in contact potential could then be measured up to $\theta = 1$. If the filament or electrode can be cooled sufficiently below the temperature of the tube, the properties of polyatomic films may be studied.

(d) The two filament method was used in the present investigation to study θ from 0.05 to unity. It may be used to study even polyatomic films which may be formed by maintaining the filament for a short time in saturated Cs vapor or by producing supersaturated vapor by rapidly heating the bulb after the filament has cooled.

Calibrations

The validity and accuracy of the various methods for determining θ were tested chiefly by observation of transient effects, i.e., phenomena involving changes in θ with time. In these tests it was assumed first that α is unity under all experimental conditions and second that the positive ion current from a clean hot tungsten filament is an exact measure of μ_a. Experimental proof of both assumptions will be given in Section XI.

If a clean tungsten filament is allowed to coat with caesium for the time t in a retarding field for ions ($\nu_p = 0$), the direct flashing method, if valid, should give measurements from which the number of atoms accumulating per cm^2 in the time t can be calculated. This number should be $\mu_a \times t$.

Fig. 4 shows data obtained by the direct flashing method with the filament at room

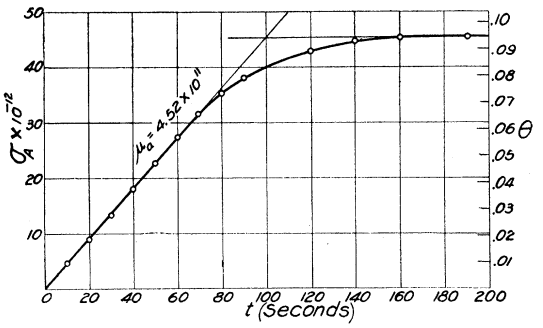

FIG. 4. Accumulation of caesium (concentration σ_A) with time as obtained by the direct flashing method. Filament at room temperature.

temperature during the accumulation period. The ordinates are σ_A (atoms cm^{-2}) as calculated from the ballistic galvanometer kicks. If Q is the quantity of electricity corresponding to the observed kick, $\sigma_A = Q/S_A e$ atoms cm^{-2}, where e is the electron charge. The galvanometer was calibrated ballistically by discharge of a standard condenser charged to a known voltage. The sensitivity was 3.3×10^{-10} coulombs mm^{-1}. The right-hand ordinates are the values of θ. Each point shown corresponds to a separate run in which Cs was allowed to accumulate for the time t after cleaning the filament by flashing.

The straight line in the figure has been drawn with the slope μ_a as given by the steady ion current. The points lie on this line within the experimental error of <1 percent for θ below about 0.07. The deviation above $\theta = 0.07$ is due to evaporation of Cs partly as atoms during the flash to obtain the ballistic kick. These curves remained unchanged if the coating temperature

was varied from 300° to 800°. At still higher temperatures, deviations set in due to the re-evaporation of arriving Cs atoms. These will be described in Section XI.

In the same way the 2-filament method was tested by measuring accumulated amounts of caesium corresponding to θ from ~ 0.05 to nearly 1.0. In this case the ballistic kick Q should equal $S_A \mu_a t f e$, where f is the fraction of the atoms intercepted by filament B. As found from the distance (2.85 mm) between filaments A and B, measured by a microscope with eyepiece scale, f was 0.0071. On plotting the observed values of σ_A, calculated from the ballistic kicks, ($\sigma_A = Q/S_A e f$), it is seen, Fig. 5, that these values

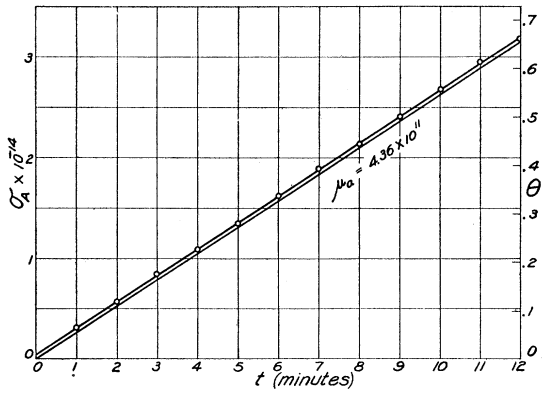

FIG. 5. Calibration of two filament method.

have accurately the calculated slope, μ_a, but are displaced slightly with respect to the calculated line. Thus the kicks extrapolated to zero time were not zero. This displacement was shown to be independent of θ and caesium pressure. A brief investigation did not reveal the cause of the displacement; it is probably connected with the pressure lags mentioned in the next section. This small empirical correction (-0.0086) was applied to all values of θ obtained by the 2-filament method.

In addition to these preliminary comparisons, later measurements of equilibrium values of θ by both the direct flashing and 2-filament methods in the range of θ from 0.05 to 0.08 were in good agreement.

Becker's method was tried out extensively and the limitations already given as to testing temperature and Cs pressure found.

IV. Description of the Experimental Tube

To obtain accurate results by the foregoing methods many precautions are necessary in the construction of the apparatus and in its use.

The caesium pressure must be exactly controlled. The ordinary construction with metal cylindrical electrodes inside a glass bulb does not allow this. These cylinders become heavily coated in the presence of caesium vapor and since their temperature is indefinite and affected by radiation from the filaments, the rate of supply of Cs is non-uniform. The use of metal electrodes deposited directly on the walls of the tube avoids this, by giving more direct thermal contact with the bath liquid.

The guard ring principle must be employed to allow measurement of currents from a known length of filament and to prevent measurement of currents from the ends or any portion of the filament which is not at the temperature of the central part of the filament. This is far more important in studies of caesium on tungsten than for clean tungsten. For example, if the central part of the filament is hot enough to be practically free from caesium, the end portions may be cooled sufficiently by the leads to have high values of θ from which the electron emission is thousands of times greater than from the cleaner central part.

The filaments should be so long that the cooling effect of the leads does not cause a non-uniform temperature over the central part even at low filament temperature.

(1) Preparation of the tube

Fig. 6a shows the glass mantle. The two annular folds (E) were made by pressing together while hot two enlarged sections of the tube. These folds divide the tube into three sections, c_1, c_0 and c_2, spaced $\sim \frac{1}{2}$ mm apart, which later are to serve as electrodes. The connections to each electrode consist of tungsten seals from which 5 mil platinum wires are led to and are partially imbedded in the glass wall.

In Fig. 6a, P is the 10 mil platinum filament in place ready for the coating of the walls by evaporation. The tube at this stage was evacuated and baked at 400°C for 2 hours, after which the oven temperature was lowered to

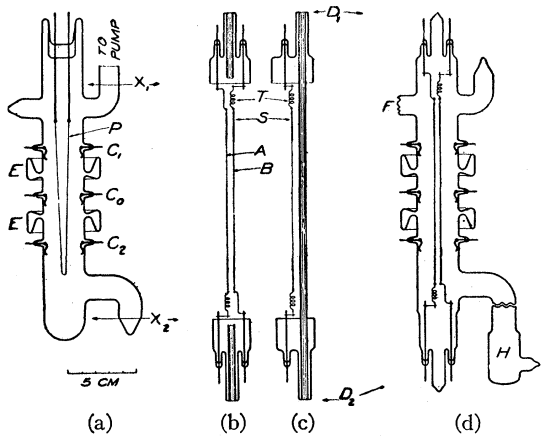

FIG. 6. Preparation of the experimental tube. (a) Outer glass mantle with platinum filament for coating walls. (b) Frame on which the filament structure is mounted and inserted in outer tube. (c) Frame turned through 90°. (d) The completed tube.

about 300°C. The filament was now heated to a temperature where the evaporation of platinum in a period of about two hours was sufficient to coat the glass walls with a film whose resistance as measured between the pairs of leads to each section was less than 50 ohms. Since the greater part of each annular fold received no platinum in this evaporation process, these folds now acted as insulation between the three electrodes, c_1, c_0 and c_2. In addition these folds could later be conveniently heated by a few turns of resistance wire to prevent electrical leaks which otherwise often occurred at the higher caesium pressures.

(2) Preparation of the filament structure

Since the filaments A (2 mil) and B (5 mil) must be accurately and uniformly spaced, they were first mounted on a frame as shown in Fig. 6b. This frame consisted of two pairs of glass seals (with tungsten leads) separated by a rigid glass rod. Fig. 6c shows the frame turned through 90°. The filament structure was adjusted and aligned entirely on this frame. The total length of each filament was 30 cm while the length of the central part in cylinder c_0, was 3 cm. To obtain this length of 30 cm more conveniently, the ends of each filament were wound into tight spirals, (S), the 2 mil filament being wound on a 3 mil mandrel and the 5 mil on a 5 mil mandrel, leaving a straight length of 10 cm between the spirals. By trial the tension springs (T) were selected and stretched so that when heated the filaments remained taut and did not shift laterally.

(3) Complete assembly

Now the platinum coating filament was removed at X_1 and the tube also opened at X_2. The frame carrying the filaments was next inserted, lower end (of smaller diameter than the inside of the main tube) first. It was sealed at X_1 and X_2 after which the glass rod having fulfilled its purpose was removed and its supporting tubes sealed off at D_1 and D_2. The filaments remained as previously adjusted. Fig. 6d shows the completed tube. The tube, with charcoal tube and ionization gauge attached at F, was then evacuated, rebaked and tested with the gauge for leaks and slow evolution of gas. The charcoal tube was separately outgassed at a higher temperature. Just before sealing off, a thin walled glass capsule of caesium was broken in a side tube and about one cc of caesium distilled into the large appendix H. The usual gas evolution in this process was avoided by using capsules filled with caesium which had already been well freed from gas.

The filaments A and B were 2.85 mm apart as determined by examination with a microscope through the clear glass annular folds. From this spacing and the known diameters of A and B, the fraction (f) of the atoms leaving A which are intercepted by B was calculated. $f=0.0071$.

Aging of tungsten filaments

In previous work on the electron emission from clean tungsten it has been found necessary to age the filaments to obtain reproducible results. With Cs on W an aging process is perhaps even more important. All filaments used were aged at 2400°K for at least 10 hours followed by an hour at 2600° and finally several short flashes at 2900°. It was further shown that the rate of evaporation of Cs ions from the filament was a most sensitive guide in this process. The cold filament was allowed to coat with Cs, the tube being at room temperature. The tube was then immersed in liquid air to freeze out all Cs vapor. Next the filament was heated to a temperature (about 850°K) where the rate of ion evaporation was slow enough to be followed

on a sensitive galvanometer. If the filament were not sufficiently aged, the plot of evaporation rate against time or against the amount of Cs, θ, left on the surface at any time, showed a number of maxima or peaks as in Fig. 7. These

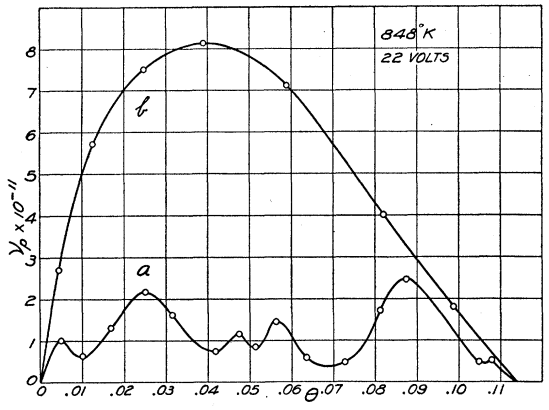

FIG. 7. (a) Irregular evaporation rate for ions from an unaged filament. (b) Uniform variation of evaporation rate from a sufficiently aged filament.

peaks were also observed by Kingdon in earlier unpublished work. Such irregular evaporation is probably caused by non-uniformities of the tungsten surface and would make it difficult to obtain rates and heats of evaporation characteristic of the whole surface. After sufficient aging, the rates of evaporation increased to maximum values and the peaks merge into a smooth curve as also shown in Fig. 7. Further aging produces no change. It was found that a fine grained filament was most easily brought into this final condition and such filaments were used in this work. The average grain size in these filaments was about one-fifth the diameter of the wire.

Control of μ_a

In these experiments μ_a was varied about one thousand-fold from $\sim 10^{11}$ to 10^{14} atoms cm^{-2} $sec.^{-1}$. To maintain any particular pressure a large Dewar flask containing kerosene vigorously stirred surrounded the tube. The bath was heated electrically or cooled below room temperature by use of a coil containing liquid air. In preliminary experiments only the appendix H was immersed in the bath, the rest of the tube being at room temperature. It was then observed that the galvanometer readings following ballistic kicks, especially at high θ's, did not return immediately to zero, but showed a lag of several seconds. This lag was found to be due to the burst of atoms suddenly liberated from filament A. These apparently did not come instantly to equilibrium with the walls of the tube and there resulted a pressure increase of short duration which was registered on filament B. This effect was eliminated by freshly coating the walls of the tube with caesium before any daily series of experiments and by immersing the whole tube in the bath liquid. This served to cover and keep covered any spots on the walls of the tube which were not acting as true caesium surfaces.

Filament temperatures

The filament temperatures were found from the known diameter and the measured value of filament current. The temperature scale for tungsten and the tables given by Jones and Langmuir[8] were used.

Below $\sim 550°$, even with the long filament used, cooling of the central part of the filament A became appreciable, because of conduction from the leads at bath temperature. Below, $\sim 750°K$, an increase in filament temperature due to radiation received from filament B (1200°) sets in.

The lead cooling correction was calculated[9] and it was shown that though the temperature of the 3 cm long central part of the filament was reduced, the distribution remained uniform to $<1°$. The lead loss correction was $-3°$ at 550°K and $-20°$ at 430°K, the lowest temperature used in measurements of atom evaporation.

The radiation correction was determined in two ways. First the change in resistance of the filament A was observed with B hot and cold, at various temperatures of A. Second, the current required to produce a given electron emission (μ_a constant) when filament B was hot and cold was observed. By comparison the true temperature of A with B hot was obtained. The radiation correction amounted to $+3°$ at 750°K and $+50°$ at 430°K.

[8] H. A. Jones and I. Langmuir, G. E. Rev. **30**, 310, 354 (1927).

[9] I. Langmuir, S. MacLane and K. B. Blodgett, Phys. Rev. **35**, 478 (1930).

V. Determination of σ_{A1}

Various low pressures ($\mu_a = 10^{11}$ to 10^{13}) of caesium were established and then filament A was maintained at a low temperature T_1 until trial showed that σ_A had reached its limiting steady value fixed by the balance between evaporation and condensation. In successive experiments, as T_1 was progressively lowered, it was found that σ_A, as given by the 2-filament method, increased at first rather rapidly and then very slowly until finally when T_1 was reduced below about 325°K no further increase in σ_A occurred. This quite definite limiting value which was observed in numerous experiments was presumed to be the value σ_{A1} corresponding to a complete monatomic film. These experiments gave $\sigma_{A1} = (4.80 \pm 0.05) \times 10^{14}$ atoms cm^{-2}.

Intervals at higher temperatures (~400°K) to allow possible favorable rearrangements by migration did not change σ_{A1}. Only by cooling the filament (by immersion of leads in liquid air) below the temperature (bath temperature) corresponding to saturated caesium vapor were other values of σ observed. These were greater than 4.8×10^{-14} and increased very rapidly as the filament was cooled below bath temperature. If the filament was now heated only slightly above bath temperature, $\sigma_{A1} = 4.8 \times 10^{-14}$ was again obtained.

In these experiments no detailed study was made of the conditions which give values of σ_A slightly lower than σ_{A1}. In later experiments, Section XII, the actual slow variation of σ with T and μ_a in this region was recorded and further justification is given for regarding this limiting value as that corresponding to a complete monatomic film.

VI. Analysis of Experimental Data on Atom Evaporation

Fig. 8 gives the experimental data on atom evaporation. The apparent (observed) concentration of adsorbed caesium, σ_A, is plotted as a function of $1/T$. For each curve μ_a is constant and has the value indicated. The values of σ_A above 0.25×10^{14} were determined by the 2-filament method. Below 0.30×10^{14}, σ_A was determined by the direct flashing method. An enlarged plot of the lower σ_A data is also given.

The equation chosen for analysis of the data is

$$\ln \nu_a = A_a - B_a/T, \tag{6}$$

where A_a and B_a were functions of θ only. It has been shown theoretically[2] that A_a consists of two parts such that

$$A_a = A + S, \tag{7}$$

where

$$S = \ln \theta + 1/(1-\theta) - \ln (1-\theta). \tag{8}$$

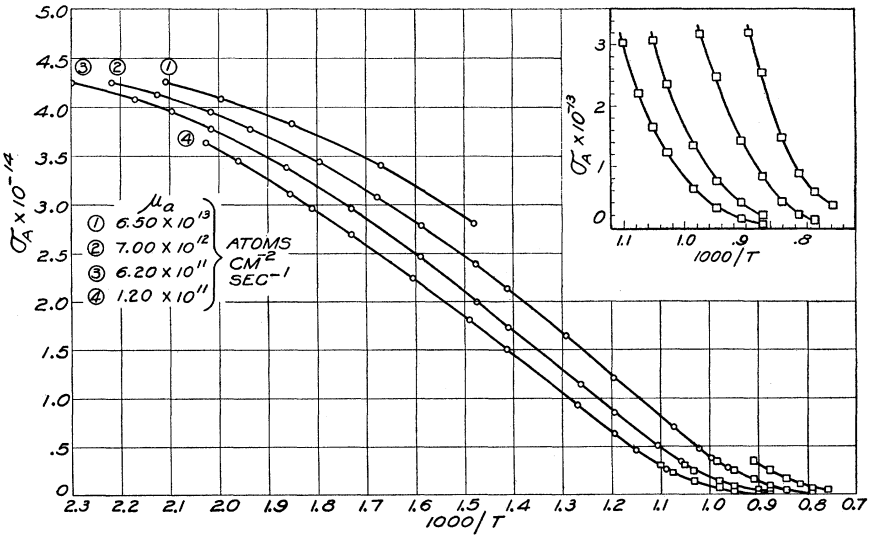

FIG. 8. Experimental data on atom evaporation. Observed concentration of caesium (σ_A) as a function of $1/T$.

The dependence of A and B_a on θ remained to be determined by the experiments.

If this form of equation is applicable to the observed data, then $(\ln \nu_a - S)$ plotted as a function of $1/T$, at any value of θ, should give straight lines of slope B_a and intercept A. With the values of $\nu_a (=\mu_a)$ and $1/T$ at various constant values of σ, read from the smooth curves (Fig. 8) drawn through the experimental points, such straight lines were obtained. The intercepts, A, showed a small variation with θ expressed empirically by

$$A = 61 + 4.8(\theta - \tfrac{1}{2}\theta^2). \tag{9}$$

With values of A and S from Eqs. (9) and (8) A_a was calculated as a function of θ. From these values of A_a and the observed values of ν_a and T from the data shown in Fig. 8, B_a was calculated by Eq. (6). For values of θ up to about 0.6, it was found empirically that B_a for all values of μ_a could be represented by

$$B_a = 32{,}380/(1 + 0.714\theta) \tag{10}$$

within the experimental error of about 0.3 percent. For larger θ's, B_a deviated from this expression slightly; however, the deviation was about 2 percent at $\theta = 0.8$ and 4 percent at $\theta = 0.9$.

The extent of the agreement of the values of B_a obtained from the experimental data with the empirical equation, Eq. (10), is shown in Fig. 9 which is a plot of $1/B_a$ against θ. If the data are to agree with Eq. (10), the points should lie on a straight line.

In the first analysis of the data by this method, values of $1/B_a$ were obtained which fitted Eq. (10) down to $\theta = 0.05$. Below this $1/B_a$ deviated as shown at X in Fig. 9. Such a deviation means that the observed values of ν_a were less than those calculated by Eq. (6) when using values of B_a from Eq. (10). At such low surface concentrations, repulsive forces between adatoms should begin to be inappreciable so that the equation of state of the adsorbed film on a *homogeneous* tungsten surface should approach that of an ideal 2-dimensional gas, *viz.*, $F = \sigma kT$. This would mean that the heat of evaporation measured by B_a should change very little with θ for these small values of θ. It seems possible to account for the increasingly rapid

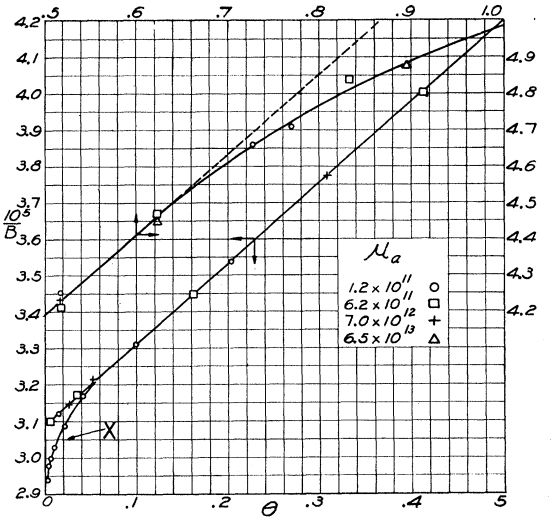

FIG. 9. Experimental variation of $1/B_a$ with θ. B_a is proportional to the heat of evaporation for atoms. X is the deviation caused by the active areas.

change in B_a at low θ as shown by curve X, only if the tungsten surface is not completely homogeneous. By trial it was found that this difficulty disappeared if it was assumed that 0.5 percent of the tungsten surface holds caesium so much more firmly than the rest that this *active surface* becomes saturated before more than 0.5 percent of the remaining surface is occupied. Thus the total concentration could be expressed as

$$\sigma_{\text{obs}} = \sigma_a + \sigma_n = \sigma_{A1}(\theta_a + \theta_n), \tag{11}$$

where the subscripts refer to the active and normal parts of the surface. When the active surface becomes saturated, so that $\theta_a = 0.005$,

$$\theta_n = \theta_{\text{obs}} - 0.005. \tag{12}$$

Calculating ν_a or $1/B_a$ from Eqs. (6) and (10) with θ_n instead of θ_{obs} gave agreement with experiment down to values of θ_n as low as 0.01, as shown by the points that lie along the straight line in Fig. 9. Any deviations which existed below this concentration were to be attributed to lack of saturation of the active surface, i.e., when $\theta_a < 0.005$.

The validity of Eqs. (6), (9) and (10) and likewise the precision of the experimental determinations of θ, is shown by the fact that the experimental points in Fig. 8 have an average deviation from the calculated curve of about 1°

in T with no deviation greater than 3° up to $\theta \backsimeq 0.6$; at higher θ's the deviations vary from 2 to 15°.

For convenience in calculation, Eq. (6) may be written with common logs as

$$\log_{10} \nu_a = \mathbf{A}_a - \mathbf{B}_a/T \qquad (13)$$

where $\mathbf{A}_a$ and $\mathbf{B}_a$ in heavy faced type represent the values of A_a and B_a (from Eqs. (7) and (10)) divided by 2.303. Table I in the first two columns contains values of $\mathbf{A}_a$ and $\mathbf{B}_a$. Up to $\theta = 0.6$ the tabulated values of $\mathbf{B}_a$ were calculated from Eq. (10). At higher θ's the experimental variation of $\mathbf{B}_a$ with θ was used as determined from Fig. 9. Complete explanation of the use of Table I will be given in Section X after electron and ion emission have also been discussed.

Fig. 10 shows θ_n as a function of $1/T$ (calculated through Table I) for a large range of values of μ_a.

TABLE I. *Data for calculation of evaporation rates.*
$\text{Log}_{10}\, \nu = \mathbf{A} - \mathbf{B}/T$

(Note that here common logs are used. To obtain values of A_a and B_a for use in Eqs. (6) to (10) multiply the tabulated values by 2.303.)

	Atoms (ν_a)		Ions (ν_p)		Electrons (ν_e) $\mathbf{A}_e = 27.55$	
θ_n	$\mathbf{A}_a$	$\mathbf{B}_a$	$\mathbf{A}_p$	$\mathbf{B}_p$	$\mathbf{B}_e$	V_c
0		14061.2		10293.6	23990	0.000
0.002	24.2328	14043.2	23.9318	10409	23853	.0268
.005	24.6401	14013.3	24.3391	10515.6	23716	.0540
.01	24.9558	13963.8	24.6549	10730.1	23452	.1064
.02	25.2859	13866	24.9849	11141.8	22941	.2079
.03	25.4913	13769	25.1904	11530	22457	.3038
.04	25.6459	13673	25.3450	11898	21992	.3960
.05	25.7719	13579	25.4709	12248	21549	.4840
.06	25.8804	13486	25.5795	12582	21122	.5686
.07	25.9764	13394	25.6755	12894	20719	.6487
.08	26.0633	13304	25.7623	13196	20325	.7267
.10	26.2179	13127	25.9169	13761	19584	.8738
.12	26.3556	12954	26.0546	14284	18888	1.012
.15	26.5388	12703	26.2379	15029	17893	1.2094
.20	26.8081	12306	26.507	16095	16429	1.500
.25	27.050	11934	26.749	17061	15089	1.7658
.30	27.276	11583	26.975	17907	13891	2.0034
.40	27.707	10939	27.406	19365	11792	2.420
.50	28.142	10364	27.841	20350	10230	2.73
.55	28.375	10098	28.069	20588	9726	2.83
.60	28.629	9849	28.328	20638	9424	2.89
.65	28.916	9623	28.612	20563	9272	2.92
.70	29.256	9425	28.955	20368	9272	2.92
.75	29.683	9256	29.377	20103	9373	2.90
.80	30.266	9110	29.965	19800	9524	2.87
.85	31.159	8985				
.90	32.821	8881				
.95	37.495	8798				
1.00		8733				

Theory of adsorption by isolated active spots

If the isolated active areas are all alike and each is capable of holding only one adatom, the average life τ_a of an adatom on the active area is independent of σ_a. Since the probability per second for the evaporation of any adatom is

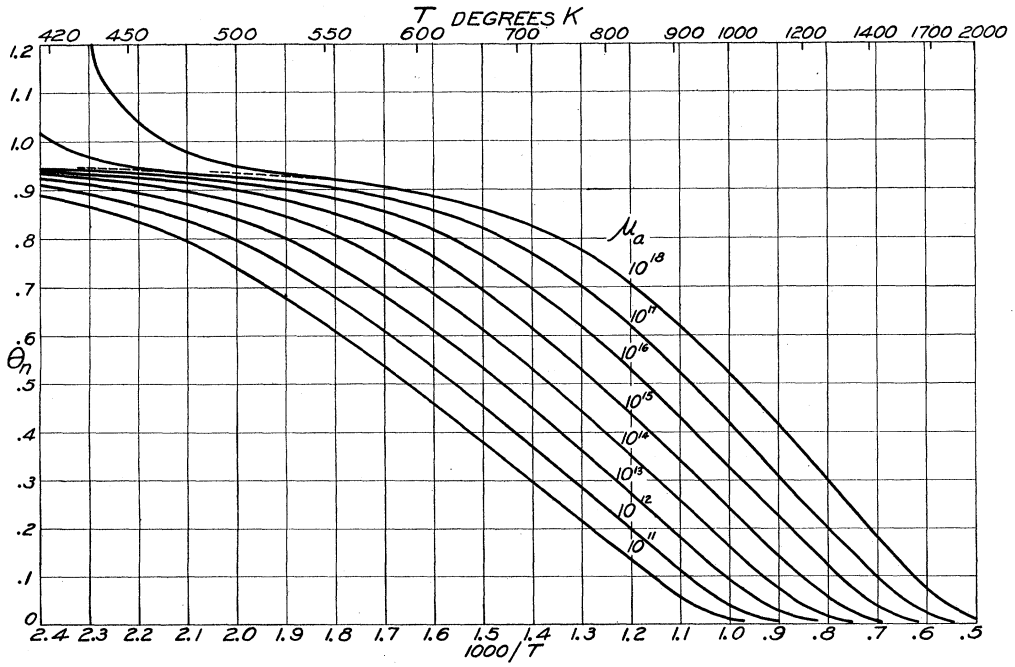

FIG. 10. Fraction (θ_n) of the tungsten surface covered with caesium at the temperature T; calculated (Eq. (6) or Table I) for different μ_a's. μ_a is proportional to caesium pressure.

$1/\tau_a$, the total rate of evaporation from the active areas is σ_a/τ_a.

In a steady state this must be balanced by the rate of arrival of adatoms from the vapor phase. Since α for the surface as a whole is unity, we must assume that an incident atom whose path is directed towards an elementary space of the active area which is already occupied by an adatom, condenses in an adjacent vacant normal space. The total rate of arrival into the active areas from the vapor phase is thus $\mu(\theta_{a1}-\theta_a)$, where θ_{a1} is the maximum value of θ_a. Equating the rates of evaporation and condensation we have

$$\mu(\theta_{a1}-\theta_a)/\theta_a=\sigma_{a1}/\tau_a. \quad (14)$$

Langmuir has derived a general equation for the life of adatoms which may readily be put in the form[10]

$$\tau/\sigma_{a1}=1.73\times10^{-27}M^{\frac{1}{2}}T_M^{-1}\epsilon^{b/T} \quad (15)$$

where T_M is the mean temperature over the range of validity of the equation. Taking $T_M=800°$ and $M=133$ (the atomic weight of Cs) and eliminating σ_{a1}/τ_a between this equation and Eq. (14) we obtain

$$\ln[\mu(\theta_{a1}-\theta_a)/\theta_a]=65.8-b/T.$$

With common logarithms this becomes

$$\log_{10}[\mu(\theta_{a1}-\theta_a)/\theta_a]=28.58-\mathbf{B}'/T. \quad (16)$$

In these equations θ_{a1} and $\mathbf{B}'$ should be constants whose values we now wish to determine from our experimental data on θ_{obs} as a function of μ and T for very dilute caesium films. These data are given in the first three columns of Table II.

TABLE II. *Relation of adsorption on active and on normal areas for dilute caesium films.*

1 μ_a	2 θ_{obs}	3 $10^3/T$	4 $\mathbf{A}_a$	5 $\mathbf{B}_a$	6 θ_n	7 θ_a	8 θ'	9 $\mathbf{B}'$
1.2×10^{11}	.00209	.891	23607	14059	.00048	.00161	.322	19306
	.00419	.925	24076	14050	.00141	.00278	.555	19020
	.00628	.945	24345	14037	.00257	.00371	.742	19000
7.0×10^{12}	.00209	.775	23739	14058	.00065	.00144	.288	19797
	.00419	.810	24219	14043	.00195	.00224	.448	19328
	.00628	.828	24461	14030	.00337	.00291	.582	19188
	.01047	.850	24744	14000	.00630	.00417	.835	19388

[10] See reference 2. The above Eq. (15) is obtained by combining Eqs. (5), (6), (7) and (37) on pages 2799 and 2806.

A series of trials has shown that the best agreement of these data with Eq. (16) is obtained if we take $\theta_{a1}=0.005$ as found in the preliminary analysis which led to Eq. (12).

Since μ can be expressed as a function of θ_n and T by Eqs. (6) to (10) or by Table I, we can by a series of approximations (or graphically) determine θ_n for each set of experimental values of μ and T. The values calculated in this way are given in the 6th column of Table II. Columns 4 and 5 contain values of $\mathbf{A}_a$ and $\mathbf{B}_a$ used in these calculations.

Subtracting θ_n from θ_{obs} in accordance with Eq. (12) we obtain the values of θ_a given in the 7th column. The 8th column contains θ', the fraction of the active surface occupied by adatoms:

$$\theta'=\theta_a/\theta_{a1}=200\theta_a.$$

The 9th column contains values of $\mathbf{B}'$ calculated from Eq. (16) from the values of μ, θ_a, and T in the table. These results fully justify our assumption that $\mathbf{B}'$ is independent of θ_a and indicate that the adatoms in the active areas are so far apart that they do not influence one another and therefore are to be regarded as isolated active spots. Eq. (16) becomes

$$\log_{10}[\mu(1-\theta')/\theta']=28.58-19{,}300/T. \quad (17)$$

These "active" spots may be located at any reentrant angle between crystal planes or at irregularities in the lattice which may cause a Cs atom to be held more tightly than at other points. Thus the active area θ_{a1} will probably vary in extent depending on the grain size of the filament and on the heat treatment given. However, the properties of the normal surface will be unaffected. It is to be noted that Eq. (17) is in such a form as to be valid even if θ_{a1} should change.

VII. Equation of State and Evaporation Equation for the Adsorbed Cs Film

The equation of state of the two dimensional gas making up the adsorbed film was found theoretically[2] for molecules which repel as dipoles, by means of the Clausius virial. The forces are repulsive forces varying as the inverse 4th power of the distance (r) between adatoms. This equation gave the spreading force F in

terms of θ, T, and the dipole moment M. By use of Gibbs' equation for the adsorption isotherm, the rate of evaporation of atoms ν_a could be expressed in terms of θ, T, and the spreading force F. These equations were of the form required by the experimental data. Therefore F and hence M could be calculated as functions of θ entirely from data on the evaporation of atoms.

The contact potential of the surface against that for pure tungsten could also be calculated from the relation.

$$V_c = 2\pi M\sigma(\text{c.g.s.}) = 1885 M\sigma_1\theta \text{ volts.} \quad (18)$$

After obtaining V_c, the electron emission ν_e was calculated for any value of θ from the Boltzmann equation,

$$\nu_e/\nu_w = \exp\,(V_c e/kT) \quad (19)$$

and Dushman's equation for ν_w, the electron emission from clean tungsten.

Likewise the rate of ion evaporation, ν_p, was calculable[11] with the aid of the Saha equation and was given by

$$\ln\,(2\nu_p) = \ln\,\nu_a + (e/kT)(V_w - V_i - V_c) \quad (20)$$

where V_w is the electron affinity of pure tungsten 4.62 volts, V_i is the ionizing potential of the caesium atoms 3.874 volts, and V_c is the contact potential as defined above. Thus from data on neutral atom evaporation (ν_a, θ, T) it was possible to calculate M, V_c, ν_e, and ν_p for comparison with the experimental values of these quantities. Further details and a tabulation of the calculated values of F, M, V_c, and other quantities included in the theoretical equations are given in reference 2.

VIII. Contact Potential and Electron Emission (Experimental)

The electron emission, ν_e, was measured from filament A at various filament temperatures and pressures of Cs. The relation between θ and pressure being known, the θ corresponding to each emission was also known. As a check in part of the runs, θ was determined immediately following the measurement of ν_e, by flashing to filament B (2-filament method).

The values of ν_e involved in the calculation of contact potentials from the Boltzmann Eq. (19) and for use in equations relating ν_e to ν_a and ν_p, must correspond to thermodynamic equilibrium and hence were measured at zero field. The effect of the external field on the electron emission from Cs coated tungsten is in general larger than for pure tungsten and varies with θ. Current-voltage data were taken for a series of constant temperatures and constant values of Cs pressure, corresponding to values of θ from 0.16 to 0.80. As shown in Fig. 11 there were sharp breaks in the plotted data and the value of ν_e at the break was taken to represent ν_e at zero field. The great variation of the effect with θ is readily seen. Fig. 12 shows that at high and low values of θ the variation of ν_e with voltage approaches that for clean tungsten. The largest departure is near $\theta = 0.55$ and decreases rapidly beyond a θ of about 0.65. The slopes below θ's of 0.30 were not measured accurately enough to

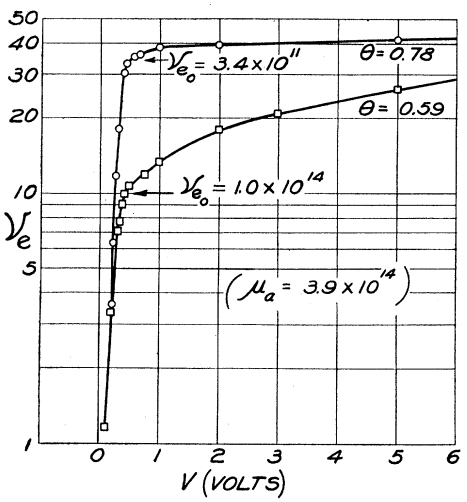

FIG. 11. Electron emission (ν_e) *vs.* voltage for Cs on W. Example of curves used to determine ν_e at zero field.

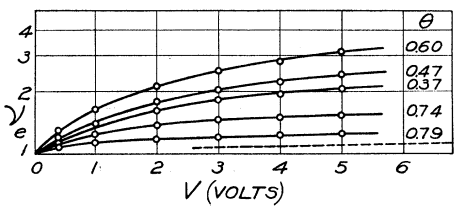

FIG. 12. Change of effect of external field on ν_e with θ. Dotted line indicates slope of curve for pure tungsten, $\theta = 0$.

[11] See reference 2, pages 2825–2826.

show how rapidly the behavior of clean tungsten was approached at low θ. It should also be noted (Fig. 13) that the zero-field emission as obtained in this way may be far lower than that value obtained by extrapolating the normal higher voltage range Schottky slope to zero field as Dushman has done.[12]

To compare these electron emission data with the values calculated from experiments on atom evaporation as described in Section VII, the corresponding values of the contact potentials against a pure tungsten surface are plotted in Fig. 14 as functions of θ. The heavy line curve

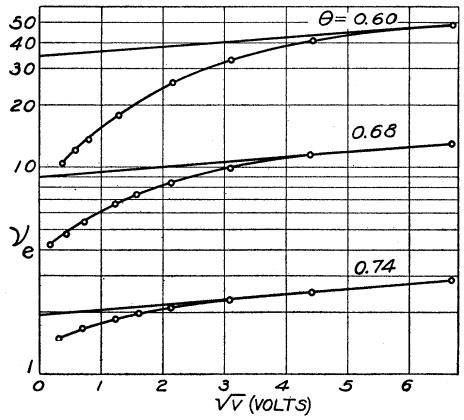

FIG. 13. Theoretical Schottky slope (straight lines) compared to actual course of current-voltage curves as zero field is approached.

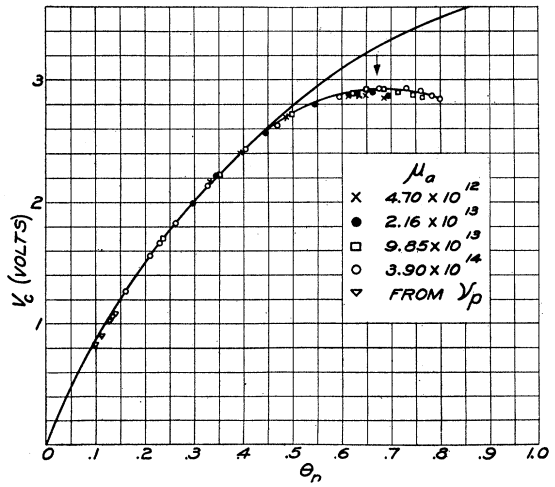

FIG. 14. Contact potential V_c. Variation with θ as determined from measurements of ν_e given by circles, etc. V_c from measurements of ν_p given by triangles. Values calculated from atom evaporation data given by heavier solid curve.

[12] S. Dushman, G. E. Rev. **26**, 157 (1923).

is calculated from data on ν_a by the methods described in Section VII, by using a temperature of 800°K. The values obtained with $T=600°$ or $T=1000°$ are practically identical with those at 800° (within about 0.02 volt for V_c). The points indicated by circles, etc., are the contact potentials calculated by Eq. (19), from the ratio of the observed electron emission to that from pure tungsten. The agreement is excellent up to θ of about 0.50. At this point the values obtained from ν_a deviate and show no maximum as do the points calculated from the observed electron emission. The deviation in this region is probably to be explained by a change in the law of force between adatoms as the atoms become crowded. The force varying as r^{-4}, as used in the theory, is evidently no longer adequate.

Table III contains the data on ν_e for a series of values of θ and T at four different Cs pressures, together with the contact potentials calculated from Eq. (19). Over the entire range of θ, T changed about 500°. At constant θ, ν_a varied about 100-fold and T changed 20 to 30° in going from the lowest to the highest Cs pressure. This small range of T prevents any conclusions as to the effect of temperature on the contact potentials. However, the value 2.8 volts, obtained by Langmuir and Kingdon,[13] for a heavily Cs coated filament, by direct measurement at ~300°K, suggests there is no large dependence on temperature.

It is to be noted that the maximum V_c or ν_e occurs at $\theta=0.67$ and decreases as θ approaches 1.0. As θ's of 0.5 to 0.6 are approached, the adsorbed Cs atoms begin to form a fairly continuous layer. The outer surface of the layer begins to have the properties of Cs and not those of a composite surface of Cs and bare tungsten as is the case at lower θ's. At still higher values of θ the already crowded layer tends to be compressed and the adsorbed atoms are given in effect smaller atomic volumes. In general, smaller atomic volume is accompanied by lower electron emission. This may explain the decrease in ν_e at values of $\theta>0.7$.

Since the values of contact potential from ν_a and ν_e agree so well below $\theta=0.50$, the values from ν_a have been used with Eq. (19) to construct

[13] I. Langmuir and K. H. Kingdon, Phys. Rev. **34**, 129 (1929).

TABLE III. *Data on electron emission and calculated contact potential.*

$\mu_a = 4.70\times10^{12}$				2.16×10^{13}				9.85×10^{13}				3.90×10^{14}			
T	θ	ν_e	V_c	T	θ	ν_e	V_c	T	θ	ν_e	V_c	T	θ	ν_e	V_c
774	.333	5×10^{10}	2.17	836	.298	7×10^{10}	1.99	928	.238	9×10^{10}	1.70	1050	.167	1.0×10^{11}	1.31
736	.392	3×10^{11}	2.41	801	.345	3.6×10^{11}	2.22	906	.264	2.4×10^{11}	1.85	1001	.211	2.5×10^{11}	1.56
677	.492	1.7×10^{12}	2.70	736	.443	3.7×10^{12}	2.57	836	.349	2.4×10^{12}	2.24	980	.231	4.5×10^{11}	1.66
613	.613	1.0×10^{12}	2.86	677	.545	9×10^{12}	2.80	736	.499	3.3×10^{13}	2.71	950	.263	1.0×10^{12}	1.82
604	.632	6×10^{11}	2.87	630	.631	3.8×10^{12}	2.89	677	.598	3.2×10^{13}	2.87	895	.327	6.2×10^{12}	2.14
596	.648	3.2×10^{11}	2.86	613	.663	1.5×10^{12}	2.89	661	.625	2.1×10^{13}	2.89	836	.402	3.1×10^{13}	2.43
586	.668	1.6×10^{11}	2.85	596	.696	4×10^{11}	2.87	646	.652	1.3×10^{13}	2.91	789	.467	7.6×10^{13}	2.62
578	.685	6.5×10^{10}	2.84					630	.682	5.6×10^{12}	2.91	707	.595	1.0×10^{14}	2.86
								613	.713	1.9×10^{12}	2.90	661	.673	4.2×10^{13}	2.93
								596	.745	3.7×10^{11}	2.87	630	.729	8.8×10^{12}	2.93
								586	.763	1.4×10^{11}	2.84	613	.755	2.3×10^{12}	2.93
												596	.783	3.4×10^{11}	2.86
												586	.797	1.6×10^{11}	2.85

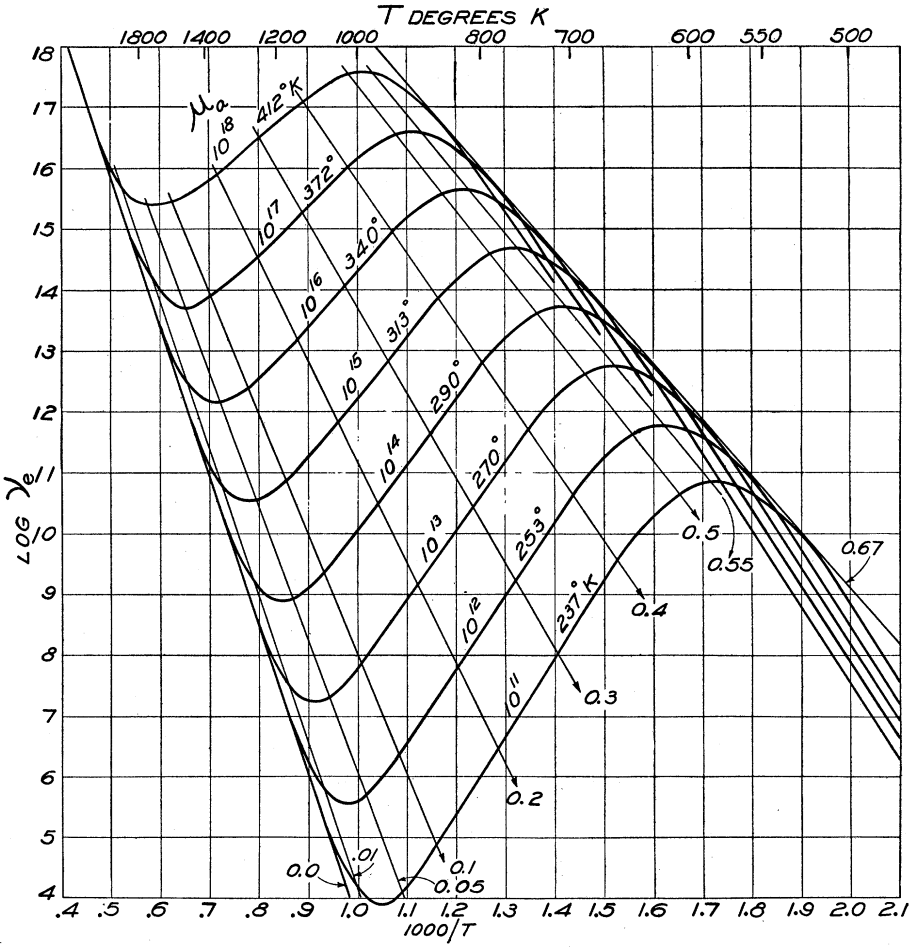

FIG. 15. Field-free electron emission (calculated) from a tungsten filament in equilibrium with Cs vapor at the filament temperature T. Rate of arrival (μ_a) of Cs and bath temperatures given on each curve. Pressure at 237°K is 6.7×10^{-7} baryes; at 412°K it is 8.8 baryes. Diagonal straight lines intersecting the curves give corresponding values of θ_n.

plots of ν_e *vs.* $1/T$ down to low values of θ. Fig. 15 shows a family of curves calculated for a series of values of μ_a. The curves were found for $\theta > 0.5$ by using the values of V_c taken from the smooth curve (Fig. 14) through the points calculated from ν_e. The highest (412°K) corresponds to a pressure of 8.8 baryes; the lowest (237°K) to 6.7×10^{-7} baryes. The curves at higher pressures may be compared with older unpublished data of Kingdon taken in the region of very low θ (0–3 percent), where the caesium emission approaches that of pure tungsten (ν_w). This is of particular interest because it may show whether the equations and constants obtained at the pressures of the present experiments can be used to calculate electron emissions at pressures many thousand times greater.

The comparison showed a difference of about 20 percent in the ratio ν_e/ν_w, the calculated values of ν_e/ν_w being lower. This is a satisfactory agreement considering the difficulty of making experiments at high pressures.

In connection with this comparison with the data of Kingdon, it is desired to correct certain equations and statements in the first paper by Langmuir and Kingdon[1] on the *Thermionic Effects Caused by Vapors of Alkali Metals*. In this work no scale of θ was available and an equation (Eq. (10), page (71)) from which θ had been eliminated was derived. This equation was to be applied in the region of very low θ. This equation in corrected form should be,

$$(\nu_e/\nu_w)^{a_1/c} \quad \ln(\nu_e/\nu_w) = (c/d)\nu_a \qquad (21)$$

derived from the two approximate equations, valid for low values of θ,

$$\ln(\nu_a/\theta) = a + a_1\theta; \quad \ln(\nu_e/\theta) = c\theta.$$

The equations representing ν_a and ν_e in the present experiments have been put in this form and the constants determined.

$$a_1 = 23{,}100/T + 6.8; \quad \ln d = 62 - 32{,}380/T$$
$$a = 62 - 32380/T; \quad a_1/c = 0.188 + 5.53 \times 10^{-5} T.$$
$$c = 123{,}000/T.$$

Calculations of ν_e or ν_e/ν_w from Eq. (21) give good agreement with the exact Eq. (19) up to θ of about 0.04. This treatment is probably applicable to dilute films in general.

In developing an equation of state, Gibbs' equation was given in a wrong form. Correctly it should be $dF/d \ln \nu_a = nkT$ as given in the present paper.

Fig. 1 in the paper by Langmuir and Kingdon shows electron emission curves plotted as in Fig. 15 of the present paper. The data of Langmuir and Kingdon were not corrected for the cooling effects of the filament leads and were not determined for zero field. Comparison of corresponding points shows emissions in Fig. 15 to be 1/3 to 1/8 of those found by Langmuir and Kingdon.

IX. Positive Ion Evaporation (Experimental)

The rate of ion evaporation was also studied as a function of filament temperature and θ at various pressures of caesium. The emission varies with field about as much as for electron emission; ν_p at zero field was obtained in the same manner as for ν_e, although (Fig. 16), the break in the log ν_p *vs.* voltage curve was not as readily determined. For this reason a slightly different method was also employed. The voltage required to keep ν_p constant as the filament temperature was varied was found to change rapidly as the

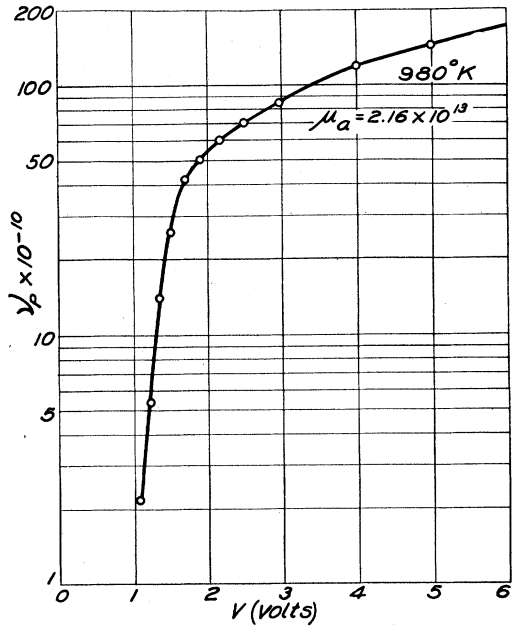

FIG. 16. Current voltage data for positive ion evaporation.

zero of potential was approached, thus allowing a closer estimate of ν_p at zero field, by choosing the point of greatest curvature. Fig. 17. Since $\mu_a=\nu_a+\nu_p$, θ could be found for any value of ν_p from the known relation between ν_a and θ. To compare with the theoretical value of ν_p, Eq. (20) was used together with $\ln \nu_{p(\text{obs})}$ to calculate the contact potential V_c. The points in Fig. 14 in the region $\theta=0.10$ to 0.14 were so calculated. The disagreement is not greater than might correspond to errors in obtaining ν_p at zero field.

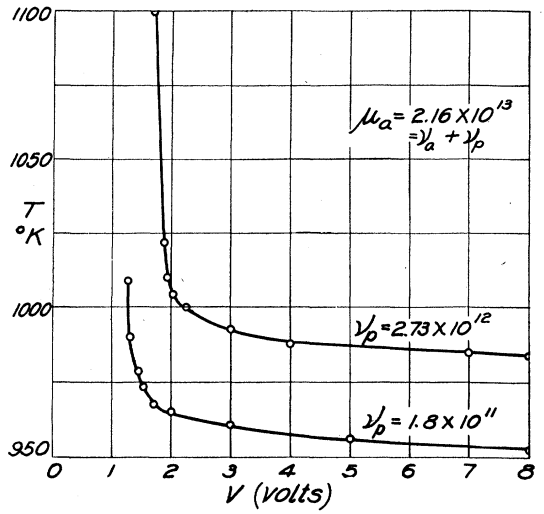

FIG. 17. Temperature voltage data for constant ν_p. Curves used to determine ν_p at zero field.

In connection with the study of positive ion evaporation rates as a function of θ, the following general characteristics of positive ion evaporation may be given.

Fig. 18 shows the exponential increase of ν_p with temperature at constant values of $\mu_a(=\nu_a+\nu_p)$. Depending on the pressure, a discontinuity sets in at a fairly definite critical temperature (which increases with μ_a) and ν_p rises at a constant rate until the value characteristic of a clean tungsten filament is reached. The variation of this maximum value of ν_p with temperature and the external field is discussed in Section XI. The discontinuity has been observed previously by Langmuir and Kingdon,[1] Killian[14] and Becker.[3] Langmuir and Kingdon[1] have shown that this discontinuity indicates the existence of caesium in two surface phases.

[14] T. J. Killian, Phys. Rev. **27**, 578 (1926).

Becker[3] was the first to point out that the existence of the two stable phases was a consequence of the relation between $\nu_a+\nu_p$ and θ.

Fig. 19 shows both atom and ion evaporation rates (calculated) in the region where ν_a and ν_p are of comparable magnitude. The full line ABC gives the sum of atom and ion rates from a tungsten filament at 848°K in caesium vapor and exposed to an accelerating field for ions.

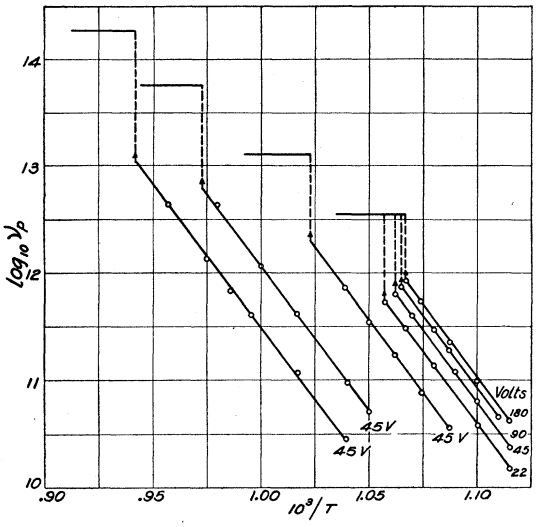

FIG. 18. Exponential increase of positive ion evaporation rate followed by discontinuous rise to maximum value of ν_p, $(\nu_p=\mu_a)$.

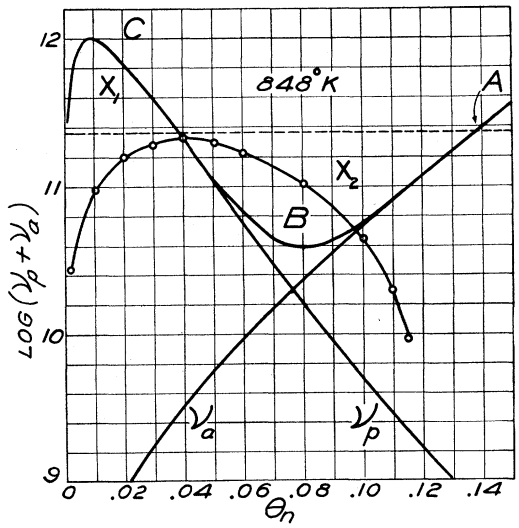

FIG. 19. Atom (ν_a) and ion (ν_p) evaporation rates for zero field at the lower values of θ. (Calculated at 848°K.) Circles give observed data under conditions as described in text.

It is seen that for constant values of $\mu_a(=\nu_a+\nu_p)$ there are three values of θ, as indicated, for example, by the intersections of the dotted line with the curve. Thus at a given pressure two values of θ may exist corresponding to two phases, a dilute (β) and a concentrated (α) phase. The intermediate θ is unstable. These phases are separated by a distinct boundary whose movement gives the observed rate of change of ν_p at the discontinuity. Migration has been shown to exist at the boundary between the phases and the velocity of propagation has been used to measure D, the coefficient of surface diffusion in a recent note[15] by the authors.

The dotted line in Fig. 19 and ABC enclose the two areas X_1 and X_2. Mathematical analysis[16] shows that the condition for a stationary boundary (when D, the surface diffusion coefficient, can be taken to be independent of θ) is that $X_1=X_2$ when $(\nu_a+\nu_p)$ is plotted as a function of θ. The dotted line in Fig. 19 has been so drawn. If μ_a is raised, the concentrated α phase will appear. The velocity of motion depends on the displacement of μ_a.

Boundaries are established by the formation and growth of nuclei at slight inhomogeneities of the surface on which θ may increase or decrease more rapidly than on neighboring areas. Nucleus growth is not possible above point A in Fig. 19 since the dilute β phase is unstable. It may and does occur for any value of μ_a producing a θ between points A and B. The μ_a or θ at which formation and growth begin depends on the surface conditions and on how rapidly μ_a (or θ) is varied.

In particular, in Fig. 18 the points where a discontinuity sets in depend entirely on this accidental nucleus formation and have no other significance. A detailed comparison of these points in Fig. 18 with the curves of Fig. 19 is difficult since ν_p in the former is affected by the field, whereas the latter curves represent field free emission of ions.

As previously discussed (Section IV), a series of ion evaporation experiments were carried out with the bulb in liquid air so that μ_a was negligible. The rate was changed by aging from an irregular to a uniform variation with θ (Fig. 7). These experiments may now be explained more fully. Since μ_a is negligible, there is no mechanism for stopping the growth of newly formed nuclei after θ's lower than those corresponding to the level of point C are reached ($\sim$0.18 percent for Fig. 19). The rate of evaporation will increase rapidly as the perimeter (boundary) of the nucleus increases, and fall off when two advancing boundaries meet. Each peak in Fig. 7 may be formed by this process. A new peak is formed as other nuclei increase their perimeters. Diffusion at the boundaries from the concentrated to the dilute phases speeds the process.

These conclusions were verified by experiments in which, after one or more peaks in the evaporation rate had been passed, the field was reversed so that only atoms could evaporate (very slowly in the region B–C). After waiting several minutes the field was again reversed and ions allowed to evaporate. The ion evaporation, however, did not proceed at the previous rate but at a rate two or three times as great. This was because θ had been made uniform, by migration from areas of high θ to those already cleared by the first peaks. A uniform low θ could also be produced by coating the clean filament in a retarding field for ions. Here again, on reversing the field, the values of ν_p were larger than when the same total θ was reached by ion evaporation.

It is emphasized that the inhomogeneities needed to serve as nuclei for these discontinuous boundary effects do not compose any appreciable part of the tungsten surface. They are probably crystal boundaries or irregularities in these boundaries and need occupy no more than the one-half percent of surface discovered in the analysis of the atom evaporation data. That the effects are not accidental, such as might be caused by gas covered areas, is shown by the exact repetition of the peaks in numbers of experiments made at any stage in the aging process. Aging probably removed certain of the inhomogeneities and caused the rest to become sufficiently uniformly distributed to produce a regular evaporation rate.

As further evidence that the smooth curve finally obtained is still disturbed by the formation and growth of nuclei and does not represent

[15] I. Langmuir and J. B. Taylor, Phys. Rev. **40**, 463 (1932).

[16] I. Langmuir, J. Chem. Phys. **1**, 3 (1933).

the true variation of ν_p with θ, the observed values of ν_p have also been plotted (circles) in Fig. 19. At higher values of θ, $\nu_{p(\text{obs})} > \nu_{p(\text{calc})}$. This is due to the formation of nuclei and boundaries as just explained. At lower values of θ, $\nu_{p(\text{obs})} < \nu_{p(\text{calc})}$. This is because the high rate of evaporation from the few remaining concentrated patches is finally overbalanced by the practically zero rate from the large areas of nearly bare tungsten. Thus the observed maximum at $\theta \sim 0.04$ and the whole behavior of $\nu_{p(\text{obs})}$ depends on the average of the rates from these two (concentrated and dilute) phases and on the displacement of the phase boundary. The surface at $\theta_{\text{obs}} = 0.04$ is made up of patches whose concentration is greater than that corresponding to $\theta = 0.04$ and areas of nearly bare tungsten.

Although the above types of experiments may give us a more detailed picture of the tungsten surface, it must be concluded that they are not suited for studies of ν_p from the main homogeneous part of the tungsten surface. As already shown, experiments made under steady conditions ($\nu_p + \nu_a = \mu_a$) do give values of ν_p in accord with theory.

The films obtained in the manner described above by evaporation of ions in accelerating fields illustrate the existence under these conditions of films which do not conform to the surface phase postulate.[17]

Killian[14] has obtained current-voltage characteristics for potassium and rubidium ions in the region of space charge limitation. He showed that the theoretical equation was followed and also gave curves exhibiting a remarkably sharp break at the saturation voltage. Figs. 20 and 21 were obtained for caesium ions and electrons in the present investigation. To avoid question as to the correct zero of potential the 2/3 power of the current has been plotted against the voltage. The break at saturation for ions is so sharp that it can be almost entirely accounted for by the small voltage drop along the central part of the filament. For electrons the transition occurs much more gradually and must have another explanation. With the masses of the

[17] A more detailed analysis of this postulate and its implications in connection with a phase rule for adsorption has been presented by I. Langmuir, in reference 16.

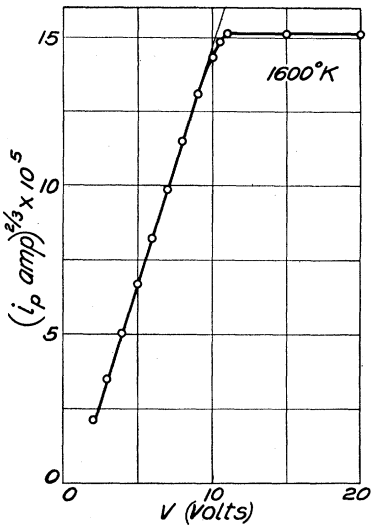

FIG. 20. Positive ion currents limited by space charge for Cs ions.

electron and of the single Cs atom, the theoretical slopes were calculated. For electrons the calculated slope was 1.14×16^{-3} and the observed 1.05×10^{-3}. For ions the calculated slope was 1.82×10^{-5} and the observed value was 1.65×10^{-5}. The agreement is satisfactory since no attempt was made to correct for the influence of the second filament held at the potential of the first in these experiments. The second fila-

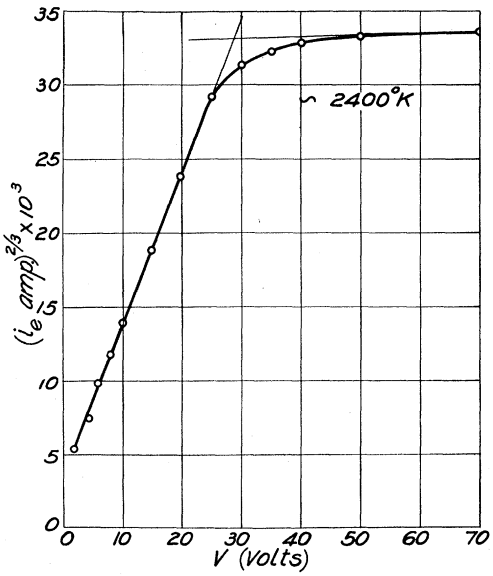

FIG. 21. Electron currents limited by space charge from clean tungsten.

ment, acting as a grid, would decrease the observed emissions and hence the slopes as found. The theoretical ratio of ion to electron slopes is 62.6 and the observed value was 63.6.

An equation, similar to Eq. (21), for the rate of positive ion evaporation at very low θ's may be developed

$$\ln(\nu_p/\theta) = b + b_1\theta,$$
$$b = 61.31 - 23{,}699/T, \qquad (22)$$
$$b_1 = 6.80 - 99{,}900/T.$$

This equation gives ν_p within one percent up to approximately $\theta = 0.02$. The limit of application is near $\theta = 0.03$ where the error is about 15 percent. By differentiation an expression giving the position of the maximum in the ν_p *vs.* θ curve is obtained

$$\theta_{\max} = T/(99{,}900 - 6.8T) \qquad (23)$$

at 500°K, 1000°K, and 2000°K, $\theta_{\max}$ is 0.00513, 0.01075 and 0.0232.

X. General Methods for Calculation of ν, θ and T

Table I has been given to simplify calculations of ν, θ and T. In the construction of this table the type of equation

$$\log_{10}\nu = \mathbf{A} - \mathbf{B}/T \qquad (24)$$

was used, where for use in the equation with common logs

$$\mathbf{A} = A/2.303 \quad \text{and} \quad \mathbf{B} = B/2.303. \qquad (25)$$

For example, A_a and B_a (for atom evaporation) refer to Eq. (1) as previously given with natural logs, $\ln\nu = A - (B/T)$. A_a and B_a have been calculated from Eqs. (7), (8), (9) and (10), which give their dependence on θ. In addition, the corresponding quantities have been calculated for positive ion emission. For ion emission,

$$A_p = A_a - \ln 2,$$
$$B_p = B_a + 11{,}606(V_c + V_i - V_w)$$
$$= B_a - 8681 + 11{,}606V_c,$$

as given by Eq. (20). For electron emission the Boltzmann equation gives $\ln\nu_e = \ln\nu_w + V_c e/kT$.

In the range 600°–1000°K the electron emission from tungsten is very closely given by

$$\ln\nu_w = 63.44 - 4.76e/kT.^* \qquad (26)$$

Therefore

$$\ln\nu_e = 63.44 - (e/kT)(4.76 - V_c)$$

or

$$A_e = 63.44, \quad B_e = 11{,}606(4.76 - V_c).$$

The contact potential (V_c) was calculated from atom evaporation data for $\theta < 0.5$ and from emission data for $\theta > 0.5$.

Here also the above values of A and B are for the equations with natural logarithms of ν, ($\ln\nu$). The **A**'s and **B**'s in Table I have been converted (by Eq. (25)) for use in the equation with logarithm to the base ten.

As an example of the use of the table, in Fig. 22, ν_a, ν_p, and ν_e have been calculated and

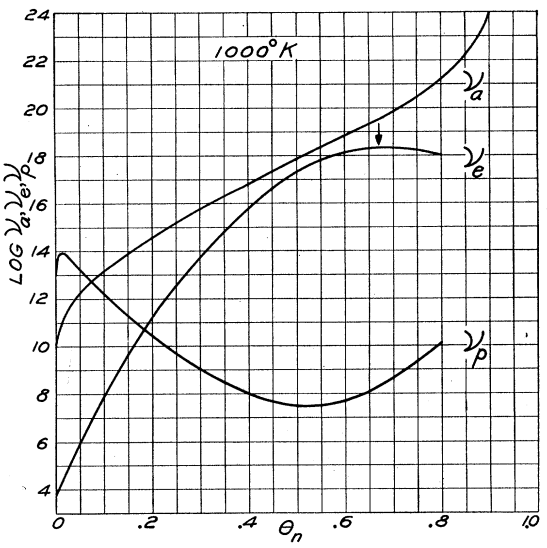

Fig. 22. Atom (ν_a), ion (ν_p), and electron (ν_e) evaporation rates at 1000°K, with zero field.

plotted as functions of θ at the constant temperature 1000°K. Fig. 19 is a similar example. Fig. 22 gives the relations between ν_e, ν_p, and ν_a as θ changes. The curves are calculated for 1000°K but their general course is similar at other temperatures.

Heats of evaporation, according to the Clapeyron equation, are given by $b_0 = -k[d\ln p/d(1/T)]$ and are obtained for atoms, ions and

* See reference 2, Eqs. (7) and (98).

electrons at any value of θ as follows:

$$b_0 = 1.987[2.303\mathbf{B} + T/2] \text{ calories}$$
$$= \frac{2.303\mathbf{B} + T/2}{11{,}606} \text{ volts},$$

where $\mathbf{B}$ is $\mathbf{B}_a$ for atoms $\mathbf{B}_p$ for ions, and $\mathbf{B}_e$ for electrons. The term $T/2$ is introduced when Eq. (24) is changed to a form containing the pressure (p) instead of the rate (ν) in accord with Eq. (5), in order to calculate b_0 as given by the Clapeyron equation. T may be taken as $T_m = 800°$, the average filament temperature in the range (600–1200°K) ordinarily used. $T/2$ corresponds at most to only a few hundredths of a volt.

The work function for electrons, i.e., the exponent (V_e) in an equation of the Dushman type

$$\nu_e = KT^2 \exp(-V_e e/kT)$$

is

$$V_e = (2.303\mathbf{B}_e - 2T_m)/11{,}606 \text{ volts}.$$

A similar equation containing $\mathbf{B}_p$ gives the work function (V_p) for ions. The term $2T_m$ corrects for the simplification made in adopting Eq. (26). Also $V_e = V_w - V_c$, where V_w is the work function (4.622 volts) for pure tungsten and V_c is the contact potential. It is to be noted that

$$V_e = (b_{oe} - (5/2)T)/11{,}606 \text{ volts}.$$

XI. The Condensation Coefficient α and Transient Phenomena

Concept of surface phase

Each phase in a heterogeneous equilibrium has properties which are uniquely determined by a definite number of parameters such as composition, temperature, pressure, etc.

If similar factors determine the properties of adsorbed films of caesium on tungsten, we may expect that all the properties of such a film would be uniquely determined by θ and T. On the other hand, one may well conceive of conditions under which the properties would depend on many other factors. For example, it is possible that the surface of the underlying tungsten may vary according to its method of preparation so that the rate of evaporation of caesium atoms from different tungsten surfaces would differ even if θ and T were the same. Or again, if a caesium film with given θ is formed in two different ways, as, for example, by condensation on to a bare surface or by evaporation from a more concentrated film, the distribution of Cs atoms over the surface might be different and thus cause variations in the properties. The properties could thus depend upon whether or not the film is in equilibrium with the surrounding Cs vapor.

It will be very useful, however, to look upon the unique dependence of the properties on θ and T as an ideal case which may be approached under favorable conditions. Let us, therefore, consider the properties of adsorbed films which conform to the following postulate.

Surface phase postulate: All the properties of an adsorbed film on an underlying surface of given composition are uniquely determined by θ and T

If this condition is fulfilled, ν_a, ν_p and ν_e are functions of θ and T only, *even if the film is not in equilibrium with the vapor phase.* The adsorbed film in equilibrium with caesium vapor is thus a system possessing two degrees of freedom in the sense of the phase rule.[16]

Under non-equilibrium conditions we then have

$$d\sigma/dt = \alpha_a\mu_a + \alpha_p\mu_p - \nu_a - \nu_p. \quad (27)$$

Case I. Retarding field for ions. Under these conditions the ions which evaporate must all be brought back to the filament surface by the field so that if there is no external source of ions,

$$\alpha_p\mu_p = \nu_p \quad (28)$$

and therefore Eq. (27) becomes

$$d\sigma/dt = \alpha_a\mu_a - \nu_a. \quad (29)$$

Under steady conditions we then have

$$\alpha_a\mu_a = \nu_a. \quad (30)$$

Case II. Accelerating field for ions. In this case $\mu_p = 0$ so that

$$d\sigma/dt = \alpha_a\mu_a - \nu_a - \nu_p. \quad (31)$$

In a steady state we have

$$\nu_p = \alpha_a\mu_a - \nu_a. \quad (32)$$

Determination of $\alpha_a\mu_a$ from the ion current

According to Eq. (32), the value $\alpha_a\mu_a$ can be calculated from the positive ion saturation current density I_p by the relation

$$\alpha_a\mu_a=(I_p/e)(1+\nu_a/\nu_p). \tag{33}$$

At high filament temperatures θ becomes very small and ν_a/ν_p approaches a limiting value which may readily be obtained from Eq. (20) by putting $V_c=0$. Inserting numerical values of V_w and V_i we thus find

$$\log_{10}(\nu_a/2\nu_p)=-3770/T. \tag{34}$$

The value of ν_p in this equation is that corresponding to zero field. In experimental determinations of I_p to measure $\alpha_a\mu_a$ we usually employed a potential of -45 volts on the cylinders. Such fields (about 3000 volts per cm at the cathode) have been shown (at constant θ) to increase ν_p about 7-fold without having any effect on ν_a. Thus the ratio ν_a/ν_p corresponding to experimental conditions should be 1/7 of that given by Eq. (34). We thus calculate that ν_a/ν_p in Eq. (33) should have values that range from 2.1×10^{-4} at $T=1200°$ to 5.8×10^{-4} at 1400°. The errors involved in neglecting ν_a/ν_p in Eq. (33) are therefore negligible.

The experimental data given in Table IV were obtained to test this conclusion. The 2nd column gives the galvanometer deflection (300 = 0.027 microampere) produced by the ion current obtained with 45 volts on the cylinder, with the filament temperatures given in the first column.

TABLE IV. *Experimental test of constancy of the ion current at high filament temperatures.*

Voltage = 45; $E=3000$ volts cm^{-1}; caesium pressure 2.4×10^{-5} baryes; $\alpha_a\mu_a=3.4\times10^{12}$.

T °K	i_p galv. defl.	i_{photo}	$i_{\text{photo}}+300.3$	θ_n
1143	300	0.02	300.3	1.2×10^{-6}
1307	300	0.50	300.8	8.6×10^{-8}
1380	302	1.5	301.8	3.3×10^{-8}
1457	305	4.6	304.9	1.3×10^{-8}
1591	325	23.1	323.4	3.4×10^{-9}
1717	381	87	387	1.1×10^{-9}
1839	560	255	555	4.6×10^{-10}

It is seen that from 1143° to nearly 1400° the current remains remarkably constant, but rises increasingly rapidly at higher temperatures. This rise has been found to be due to photoelectric emission from the adsorbed caesium film on the cylinder under the influence of the light radiated from the filament. Such photoelectric emission is also observed when light is allowed to fall on the tube.

Since the light intensity of each wave-length varies in accord with Wien's law, the logarithm of the intensity is a linear function of the reciprocal of the filament temperature, the slope of the line, for natural logarithms, being C_2/λ, where the radiation constant C_2 is 1.433 cm deg. Analyzing the data for i_p in Table IV it is found, in fact, that the observed current i_p can be resolved into two parts, one having the constant value 300.3, and the other, the photoelectric current, being given by

$$\log_{10}(i_{\text{photo}})=9.08-12{,}270/T. \tag{35}$$

The 3rd column contains values of i_{photo} calculated by this equation. The 4th column shows that the sum of these two currents, $300.3+i_{\text{photo}}$ agrees well with the observed value of i_p.

By immersing the bulb in liquid air the ion current became zero, but the photocurrents remained and were found to be 15 percent lower than those given by Eq. (35), so that the constant 9.08 in this equation needed merely to be changed to 9.01.

Repeating the experiments of Table IV, with -310 volts on the collector instead of -45, gave currents which, analyzed in the same way, gave a constant ion current having the same value (300.3) as before, but gave photocurrents 2.2 times as great as with the weaker field, the coefficient of $1/T$ in Eq. (35) being unchanged. By placing the bulb in liquid air these photocurrents were reduced as before by 15 percent.

The effective wave-length of the radiation producing these photocurrents (a kind of Crova wave-length) can be determined by equating the coefficient of $1/T$ in Eq. (35) to $2.303\times C_2/\lambda$; it is found to be 5070A, which is reasonable for caesium photoelectric cells.

We may estimate the magnitude of θ under the conditions of the experiments of Table IV by the limiting form (as θ approaches zero) of Eq. (22),

$$\log_{10}(\nu_p/\theta_n)=26.625-10{,}294/T. \tag{36}$$

Here ν_p is the ion evaporation rate without accelerating field. Since in these experiments ν_p, which was equal to μ_a, was increased 7-fold by the field, we may put $\nu_p = 4.9 \times 10^{11}$ in Eq. (36). The values of θ_n, calculated in this way, are given in the last column of Table IV. For such low values of θ, ν_e cannot differ appreciably from that for a pure tungsten surface, so that the assumptions made in deriving Eq. (34) are justified.

The experiments thus indicate that within the experimental error of about 0.2 percent the saturation ion current is independent of temperature and of field strength for ranges of temperature from 1200 to 1500° and for fields from 3000 to 20,000 volts cm^{-1}.

We must conclude from both theory and experiment that the ion saturation current method provides an extremely accurate measurement of $\alpha_o\mu_a$; where α_o is the value of α_a for very small values of θ.

Methods for the experimental determination of α_a and α_p

If, now, we had some independent means of determining the vapor pressure of caesium, from which we can calculate μ_a, we could determine α_o from our knowledge of $\alpha_o\mu_a$. However, as none of the available vapor pressure methods appears to be comparable in accuracy or sensitivity with that of the measurement of ν_p, we need to investigate other ways of finding α_a.

Experimental data, such as that of Table IV, which were also obtained for a wide range of other values of μ_a, *prove that* α_o *is strictly independent of temperature* in the range from about 1000 to 1500°, and *is independent of E, the accelerating field.* This suggests strongly that α_o is unity since any smaller value would probably vary with temperature. There are, however, other methods open to us for measuring α_a.

(1) *Direct flashing method.* Caesium is allowed to accumulate on the filament at a temperature T_1 at which ν_a is negligibly small, at the rate $\alpha_a\mu_a$. After a time t, σ_A is measured by the D.F. method (see Section III and Fig. 4). $\sigma_A = \overline{\alpha}_{av}\mu_a t$ where α_{av} is an average value of α_a over the range in θ from 0 up to the final value at time t.

Fig. 23 gives some typical data with the filament during accumulation at 300°, at 970 and 1001°.

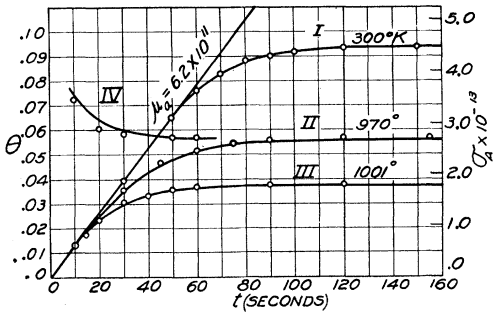

FIG. 23. σ_A *vs.* time at 300°, 970° and 1001°K, for $\mu_a = 6.20 \times 10^{11}$. Data obtained by direct flashing method for use in measuring α_a.

Each experimental point shown for curves I, II and III corresponds to a separate run in which the caesium was allowed to accumulate for the time t after cleaning the filament by flashing. The straight line drawn through the origin has been drawn with a slope equal to $\alpha_o\mu_a$ as determined by this steady ion current method. The experimentally determined points are seen to lie quite accurately on these lines at sufficiently low values of θ. We shall see that at 970 and 1001° the deviations from the straight line at the higher θ's in curves II and III agree with those calculated from the known evaporation rates of these films at those high temperatures.

The data obtained with the filament at 300°K during the accumulation time, curve I, show that the observed points lie quite accurately on the straight line through the origin up to values of θ of about 0.07. The deviations at higher θ are due to evaporation of Cs as atoms during the flashing. This is shown by the fact that the curve remains entirely unchanged if T_1 is varied from 300 to 800°K, but the deviations do depend slightly on the flashing temperature and on the rapidity with which the temperature is raised. The direct flashing method is thus only applicable for values of θ up to about 0.08.

The fact that the experimental points lie on the straight lines of slope $\alpha_o\mu_a$ for sufficiently small θ proves that $\alpha_{av}\mu_a t$ equals $\alpha_o\mu_a t$. We conclude that for temperatures up to about 800° and for values of θ up to 0.07, α_a is constant and equal to α_o within the experimental error

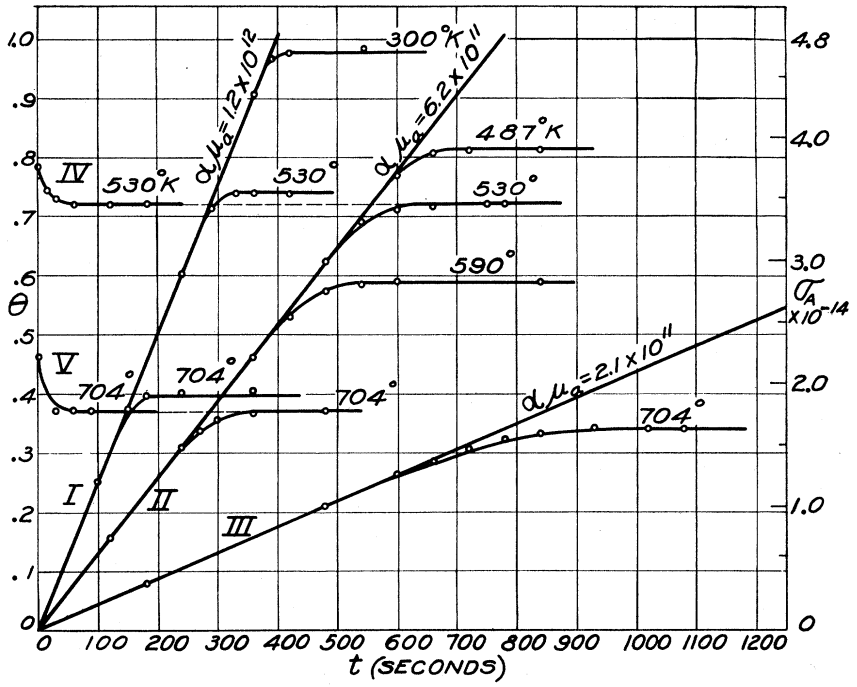

FIG. 24. σ_A *vs.* time at various filament temperatures and Cs pressures (μ_a) as indicated. Data obtained by two filament method for use in measuring α_a.

of less than 1 percent. At 970° the same conclusion may be drawn up to $\theta = 0.02$.

(2) *Two filament method.* After allowing caesium to accumulate on filament A at temperature T_1 up to a definite value of $\sigma_A = \alpha_{av}\mu_a t$, σ_A is measured by the two filament method. If Q represents the quantity of electricity corresponding to the observed ballistic kick produced when A is flashed, we have

$$Q = \alpha_{av}\mu_a t S_A f \alpha_o e, \qquad (37)$$

where S_A is the apparent surface area of the filament A within the cylinder C_o, and e is the electron charge. By dividing Q by $S_A fe$, we thus obtain values of $\alpha_{av}\alpha_o\mu_a t$.

The experimental points shown in Fig. 24 represent data obtained by this method for a series of relatively low filament temperatures, *viz.*, 300, 487, 530, 590 and 704°K and with three different caesium pressures which gave, by the steady ion current method, values of $\alpha_o\mu_a$ of 1.20×10^{12}, 2.1×10^{11} and 6.2×10^{11} atoms cm^{-2} sec.$^{-1}$.

The straight lines marked I, II and III which pass through the origin have been drawn with slopes $\alpha_o\mu_a$ as determined by the steady ion current method. It is seen that the observed points, for sufficiently low θ, lie within the experimental error on the straight lines. Since the ordinates of the experimental points are $\alpha_{av}\alpha_o\mu_a t$, while those of the straight lines are $\alpha_o\mu_a t$, this agreement proves that $\alpha_{av} = 1$ and therefore $\alpha_a = 1$ for values of θ up to 0.98. We shall see that the deviations of the observed points from these straight lines as θ approaches a limiting value, are due to evaporation and do not indicate values of α_a less than unity.

In the next section we shall discuss the theoretical significance of the experimental fact that $\alpha_a = 1$ up to nearly $\theta = 1$.

Value of α_p

Moon[18] has shown that when a beam of Cs ions (without Cs atoms) is directed against a tungsten filament heated to high temperatures, no net current flows to the filament if there is a field near the filament which draws away ions. Without this field, or at a lower filament temper-

[18] P. B. Moon, Proc. Camb. Phil. Soc. **27**, 570 (1931).

ature, a current is observed which presumably measures the number of ions which strike the filament. Moon concludes that *all* of the ions which condense on the very hot filament leave it again as ions (none as atoms). This is a proof that ν_a/ν_p is very small, but does not necessarily prove that $\alpha_p=1$, although it makes this probable. In view of the strong attractive forces between the ions and the tungsten surface (image force) it is, however, almost certain that there cannot be any appreciable reflection of low velocity ions, and we may safely conclude that $\alpha_p=1$.

Transient effects in atom evaporation

We use the term *transient effects* to describe the phenomena involving changes in θ as distinguished from *steady* states in which θ stays constant. The accumulation periods which we have discussed correspond to transient states in which ν_a and ν_p are negligible compared to μ_a. Let us now consider the theory of the changes in θ which occur when ν_a and μ_a are comparable in magnitude, and when a retarding field for ions makes $\nu_p=\mu_p$.

The data of Figs. 23 and 24 show that if a clean filament is held at constant temperature in Cs vapor of a definite pressure, θ increases at first at the steady rate μ_a/σ_{A1} but thereafter the rate decreases until finally θ approaches a steady limiting value which we shall call θ_∞. Eq. (29), which applies to this case, may be written in the following form, since $\alpha_a=1$

$$\sigma_{A1}d\theta/dt=\mu-\nu. \tag{38}$$

In this discussion we shall omit the subscripts of μ_a and ν_a except where necessary to prevent confusion.

Values of θ_∞

When $\theta=\theta_\infty$ we should have $\nu=\mu$. Thus, since by Eqs. (6) to (10) and the data of Table I, ν is given as a function of θ_n and T, we can calculate θ_n from μ and T. For each of the temperatures used in the experiments of Figs. 23 and 24 we have constructed, by the data of Table I, a curve giving ν as a function of θ_n in the range near θ_∞ and from this curve have read off the value of θ_n by taking $\nu=\alpha_o\mu_a$ as given by the steady ion current method. θ_∞ (by Eq. (12)) is then equal to $\theta_n+0.005$. The horizontal portions of the full line curves in Figs. 23 and 24 have been drawn by using these calculated values of θ_∞. The close agreement of these horizontal lines with the limiting values of θ given by the experimental points is an illustration of the accuracy of our general equations for ν_a in terms of θ and T, and serves to justify our use of the surface phase postulate.

Calculation of transient curves

By expressing ν as a function of θ and T, we can, by integration of Eq. (38), theoretically obtain θ as a function of t. The experimental determinations of ν_a have shown that ν_a at constant T increases very rapidly with θ, so that within any narrow range of values of θ, say between θ_1 and θ_2, we may put

$$\nu=K\exp(H\theta), \tag{39}$$

where K and H are constants within the range θ_1 to θ_2, but depend on the values of θ_1 and θ_2. More strictly, we may define H by differentiation of Eq. (39)

$$H=d\ln\nu/d\theta. \tag{40}$$

In Fig. 25 the ordinates are values of H calculated in this way by differentiation of the expression we have derived for $\ln\nu_a$ as functions of θ and T. It is seen that except for very small and very large values of θ, H changes relatively slowly with θ, so that the use of Eq. (39) is justified if the range θ_1 to θ_2 is not very great.

Inspection of the experimental data of Fig. 24 shows that the transition between the sloping straight line ($\sigma=\mu t$) and the horizontal straight lines ($\theta=\theta_\infty$) is very rapid. Because of the large magnitude of H, a very small decrease in θ below θ_∞ lowers ν_a to a value which is negligible compared to μ, so that $d\theta/dt$ becomes constant. Thus, to calculate the whole curve, we need only to have an expression for ν which applies to a narrow range of θ.

Introducing the value of ν from Eq. (39) into Eq. (38), we find that the final steady value θ_∞ is given by

$$\nu=K\exp(H\theta_\infty)=\mu. \tag{41}$$

Case I. If we start with a completely coated

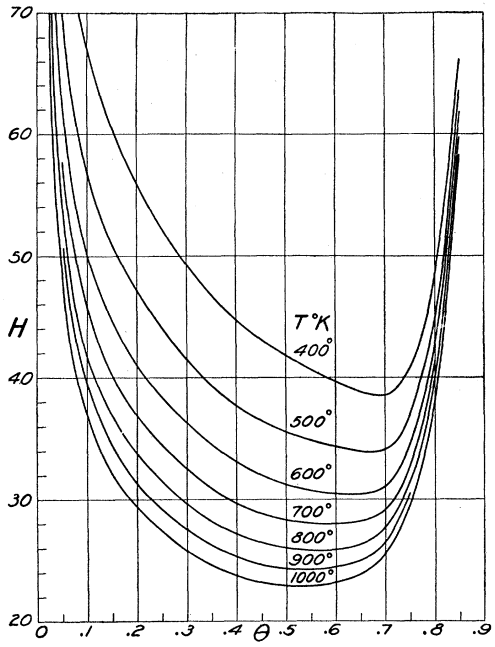

FIG. 25. Values of H, the relative rate of increase of ν_a with θ, defined by Eq. (40).

filament at $t=0$ we obtain by integration

$$\exp(-\mu Ht/\sigma_{A1}) = 1-\exp[-H(\theta-\theta_\infty)]. \quad (42)$$

Curves IV and V in Fig. 24 and curve IV in Fig. 23 are examples of Case I. For each point the completely coated filament was suddenly raised to the indicated temperatures by a condenser discharge and held there by the proper current.

The full line curves IV and V in Fig. 24 were calculated accurately by Eq. (42), by using $\mu=6.2\times10^{11}$, $\sigma_{A1}=4.8\times10^{14}$, and for curve IV, $\theta_\infty=0.72$, $H=33.9$ at 530°, while for curve V, $\theta_\infty=0.372$, $H=30.4$ at 704°. For Fig. 23 (curve IV), $\theta_\infty=0.056$ at 970°. As these values of θ_∞ were calculated from the values of μ, no adjustable parameters have been used in the construction of these curves.

Case II. Starting with $\theta=0$ at $t=0$ integration gives (if we neglect $\exp(-H\theta_\infty)$ compared to unity):

$$\exp(-\mu Ht/\sigma_{A1}) = \exp(-H\theta)-\exp(-H\theta_\infty). \quad (43)$$

The curve $OPNP'C$ in Fig. 26 is the curve given by this equation. Except for a short

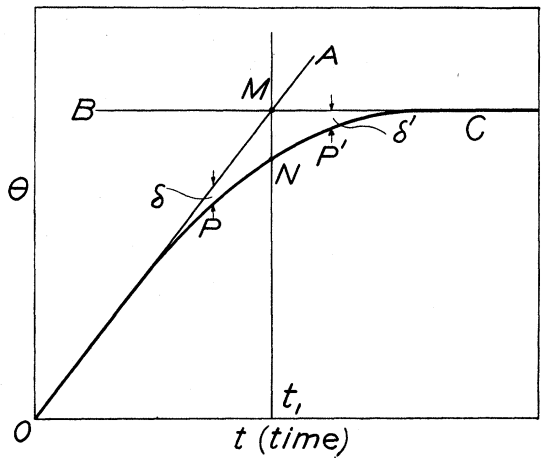

FIG. 26. Curve and construction describing Eqs. (43) to (45) used in calculation of transient curves.

transition region the curve nearly coincides with its two asymptotes OA and BC. It is therefore more convenient to express it in terms of the vertical displacement δ of a point P from the line OA or the displacement δ' from the horizontal line BC. If we let t_1 be the abscissa corresponding to the intersection M of OA and BC, our equations become

$$\exp(H\delta) = 1+\exp H\mu(t_1-t)/\sigma_{A1} \quad (44)$$

and

$$\exp(H\delta') = 1+\exp H\mu(t-t_1)/\sigma_{A1}. \quad (45)$$

Thus at points P and P', which are displaced from MN by equal horizontal distances, but in opposite directions, δ and δ' are equal. The slope of the tangent to the curve at N is one-half the slope of the line OA.

The full line curves which branch off from the lines I, II and III in Fig. 24 have been accurately calculated by these equations without the use of adjustable parameters.

The nearly perfect agreement of the points with the curves proves that the transient states during the condensation and evaporation of caesium atoms from these concentrated films are determined by the balance between the rates of condensation and evaporation as given by Eq. (38).

These experiments also prove that the surface phase postulate (S.P.P.) is applicable to these films. The agreement between the calculated curves and the experimental points show that

ν_a is determined by θ and T in accordance with Eqs. (6 to 10) and does not depend on the manner in which θ has been reached; i.e., by condensation or by evaporation.

In the transient experiments at low θ (Fig. 23) departures from the S.P.P. might be expected to occur. It has been shown that one-half percent of the surface of the filament consisted of "active spots." The final value of θ_n for 970° and $\mu_a = 6.2 \times 10^{11}$ (curve II) is calculated to be 0.051, but the plotted data show that in about 2 minutes a final value of 0.056 was reached, indicating that the active areas ($\theta = 0.005$) had been completely filled. Now in the transient state, as the filament is slowly coated, the concentrations in the normal and active areas would remain equal if there were no surface mobility by which the active areas could be filled. In 2 minutes the maximum value of θ (no reevaporation) which could be produced by the arriving atoms is ~ 0.16. However, the active areas contribute only 1/200 of this or a θ of ~ 0.0008 and without migration can be filled only after more than 12 minutes. It was particularly observed that the value of θ (0.056) reached in 2 minutes showed no increase after periods as long as 60 minutes. Also a cold filament nearly completely coated ($\theta \sim 1.0$) when heated to 970° (curve IV) quickly attained the same final value of θ leaving no doubt as to the absence of any delay in reaching a steady value of θ. The full line branching curves in Fig. 23 calculated with the assumption of complete occupation of the active spots by migration early in the coating process, agree excellently with the observed points. The existence of an *interphase surface mobility* is thus well demonstrated. It is only by virtue of such mobility[15] that the S.P.P. applies to these experiments with dilute films.

Since the surface diffusion coefficient for these films is known[15] from other experiments, it has been possible[19] to calculate the distance which the adatoms may move in reaching active spots without disturbing the surface phase equilibrium. This distance (~ 0.03 cm) was found to be large compared to the distance (~ 0.001 cm) between active spots assuming these are located along crystal boundaries.

[19] See reference 16, discussion of Eq. (12).

XII. Mechanism of Condensation and Evaporation for Concentrated Films

The fact that $\alpha_a = 1$ up to values of θ as high as $\theta = 0.98$ is of profound significance in its bearing on possible mechanisms of condensation and evaporation.

According to the reversibility principle[20] "every element in the mechanism of a reversible process must itself be reversible," so that "the mechanism of evaporation must be the exact reverse of that of condensation even down to the smallest detail."

Let us postulate several different possible mechanisms for evaporation and see whether or not, when they are reversed, they yield reasonable mechanisms for condensation and whether these are consistent with the experimental fact that $\alpha = 1$.

We first need to define some terms which will help to make our concepts more precise. In a state of equilibrium the atoms near a plane surface may be divided in general into four groups:

(1) *Adsorbed atoms or adatoms.* These are the atoms on the surface which contribute to θ.

(2) *Incident atoms*, or atoms which are moving towards the surface from remote regions. The paths described *by the nuclei* of such atoms are called *incident paths.*

(3) *Emergent atoms*, or atoms which are receding from the surface along paths (emergent paths) that will carry them to remote regions.

(4) *Hopping atoms*, or atoms whose nuclei describe paths (hopping paths) that originate and terminate on the surface.

We may define the *remote region* as that region which lies outside of the range of the surface forces, where the paths of the atoms are straight lines. The region closer to the surface where the paths are curved we shall call the *force sheath.*

When the nucleus of an incident, or a hopping atom, approaches to a definite point close to the original surface, the atom either becomes an adatom or it starts to describe a new path (emergent, or hopping). Let us call this definite point the *terminus of the path.* Similarly, each

[20] I. Langmuir, J. Am. Chem. Soc. **38**, 2221–2295 (1916). See particularly page 2253 and footnote on page 2262.

emergent and hopping path has an *origin*. The straight paths of the incident and emergent atoms in the remote region, if extended as straight lines to their intersections with an ideal plane at the adsorbing surface, give points which we shall call the *flight termini* and *flight origins*.

When equilibrium prevails, the concentration of atoms, their directions of motion, and their velocities are governed by the laws of the Maxwell-Boltzmann distribution (M.B.D.) throughout the force sheath as well as the remote region. Thus, all the paths (incident, emergent and hopping) that pass through any point have a spherically symmetrical distribution of directions at that point. The concentrations of atoms must vary in accord with the Boltzmann equation:

$$n = n_0 \exp(-Ve/kT), \tag{46}$$

where Ve is the increase in potential energy of an atom when it passes from a region where the concentration is n_0 to one at which it is n.

We see, then, that the flight termini and flight origins must be uniformly distributed over the ideal surface plane (i.e., distributed with uniform probability per unit area).

Since the adatoms are held by strong forces originating from the underlying tungsten atoms which are arranged in a definite surface lattice, there must be a strong tendency for the adatoms to occupy definite positions (elementary spaces) on the surface. Experiments on the mobility of caesium adatoms on tungsten[15] have shown that the activation energy needed to cause an adatom to hop from one elementary space to an adjacent one is about 0.6 electron-volts. Introducing this value into the exponent of Eq. (46) we find that at $T = 1000°$ the probability per unit volume for the occurrence of an atom (i.e., its nucleus) in the potential depression near the center of an elementary space is 1050 times as great as the corresponding probability for a position at the potential barrier which separates the elementary spaces.

Thus the adatoms are normally oscillating about equilibrium positions corresponding to the elementary spaces, with amplitudes which are rather small compared to the distance between elementary spaces, and only rarely hop from one position to another.

Evaporation of adatoms from dilute films

With the foregoing concept of elementary spaces, it might seem reasonable to postulate that most of the evaporating adatoms pass from their normal positions directly into the vapor phase as emergent atoms. If we think of the reverse process, however, we recognize that since the flight termini must be uniformly distributed over the surface, the incident atoms cannot in general have paths which lead them directly to the normal equilibrium positions. A large portion of the incident atoms must make their first contact with the surface in positions close to the potential barriers, and if $\alpha = 1$ all of these must then move to their final normal positions by a series of hops. Conversely, we must reason, by the reversibility principle, that a large fraction of the emergent atoms have flight origins near the potential barriers in spite of the low concentration of adatoms in these regions.

A little closer consideration shows that although at the barrier the concentration is only 1/1000th of that at the normal positions, this difference is counterbalanced by the fact that the probability of evaporation of any atom at the barrier is 1000 times as great as for an atom in a normal position. Thus the evaporation is essentially uniform over the surface, although the distribution of adatoms is nearly discontinuous.

It is thus evident, if $\alpha = 1$, that hopping paths must be enormously more numerous than emergent paths. Surface mobility is an essential part of the mechanism of evaporation.

Emergent atoms from nearly saturated films

Let us imagine a nearly saturated adsorbed film ($\theta \sim 1$) from which adatoms pass as emergent atoms into the gas phase. If this is the only mechanism of evaporation, then condensation can occur only when incident atoms make their first contact with the surface in a vacant elementary space. All other incident atoms must be reflected; that is, they must escape again by emergent paths. Hopping paths would have to be excluded, for they would provide other opportunities for condensation, and therefore there would be other mechanisms for evaporation than those which we postulated as the only possible ones.

The probability that a flight terminus shall lie in a vacant space is $1-\theta$. The probability that an incident atom should fly into a vacant space without colliding with adjacent atoms is very much less than $1-\theta$. Thus, on the basis of our assumed mechanism, α would have to be less than $1-\theta$.

An apparent reflection coefficient approaching unity for incident atoms striking a covered part of the surface may readily be accounted for by an extremely high evaporation rate from the 2nd layer of atoms as compared to that from the 1st layer.[21] It is reasonable to assume, however, that an atom cannot exist, even momentarily, in a 2nd layer unless it can be supported by four underlying adatoms in the 1st layer. The chance that a given space is occupied is θ and the chance that 4 given spaces are occupied is θ^4. Thus the probability that an incident atom will evaporate from the 2nd layer is θ^4 so that the apparent value of α would be $1-\theta^4$. Experiments with steel balls thrown at random onto a surface partly covered (to the fraction θ) with similar balls, in random arrangement in spaces which form a square lattice, show that the fraction of incident balls which go into a second layer is, in fact, very close to θ^4, for values of θ from 0.2 to 1.0. Thus for $\theta=0.85$, α would be 0.48 and for $\theta=0.98$, $\alpha=0.078$.

With this mechanism for condensation, most of the atoms which evaporate would have to make one or more collisions with the adjacent adatoms before they escape.

Although this postulated mechanism is probably suitable for the explanation of many cases of adsorption of gases on solids, it obviously is inapplicable to the case of caesium films on tungsten and all other cases in which $\alpha=1$ up to high values of θ.

With high values of θ and α the emergent atoms must come from a second adsorbed layer

Since the paths of incident atoms cannot in general be directed towards regions in which the surface concentration is below the average, it must follow, if $\alpha=1$, that just after condensation the concentration is locally raised at the point of condensation. Conversely, an atom can emerge only from regions having locally abnormally high surface concentrations and the act of emergence must bring the local surface concentration back to normal. It thus seems impossible to reconcile the observed simultaneous occurrence of high values of α and of θ with any mechanism by which an appreciable fraction of the emergent atoms have path origins in the first adsorbed layer, even if we assume a high mobility among the adatoms.

These difficulties disappear, however, if we postulate that the origins of a large fraction of the emergent paths lie in a second adsorbed layer. We must assume that adatoms in the first layer hop, from time to time, up into a second layer which, however, covers only a very small fraction of the surface. The atoms in this second layer migrate over the surface and may evaporate or may hop back into vacant spaces in the first layer. Since an atom which evaporates from the dilute film of the second layer does not leave a "hole," no difficulty occurs in assuming that all incident atoms condense by the reverse process.

Covering fraction θ_2 in second layer

We have seen that the heat of evaporation (at constant pressure) of caesium adatoms from tungsten, for values of θ approaching unity, is about 41,000 calories per gram atom, which is equivalent to 1.78 electron-volts. This, of course, represents the energy that must be expended in taking an adatom from the first layer of adatoms out to a remote region.

An atom in a second layer is not in direct contact with the tungsten surface, but is in approximately the same condition as an atom on the surface of metallic caesium. The vapor pressure p of caesium is given (in baryes) by[1]

$$\log_{10} p = 10.65 - 3992/T. \qquad (47)$$

The heat of evaporation corresponding to this equation is 18,240 calories or 0.79 volt, or only 44 percent of that of adatoms in the first layer.

The average "evaporation life" of an atom[22] in the surface of a solid or liquid is given by

$$\tau = (2\pi mkT)^{\frac{1}{2}}\sigma_1/p, \qquad (48)$$

where τ may be defined by the statement that

[21] I. Langmuir, Proc. Nat. Acad. Sci. **3**, 141 (1917).

[22] See Eq. (15), reference 2.

dt/τ is the probability that any surface atom will evaporate in the time dt. Placing $\sigma_1=3.56\times10^{14}$ we thus find that for Cs atoms in the temperature range from $T=300$ to 1100°, τ is given in seconds by

$$\log_{10}\tau=-12.82+3840/T. \tag{49}$$

Let us now assume provisionally that τ is the same for all exposed adsorbed atoms in the 2nd (or 3rd) layer on tungsten as for atoms in a surface of metallic caesium at the same temperature. We thus take τ to be independent of the surface concentration of atoms although for the 1st adsorbed layer on tungsten the strong repulsive dipole forces between adatoms cause τ to decrease as θ_1 increases. Since Cs atoms on a layer already covered by caesium probably have very small dipole moments, and any small moment that does exist may be compensated for by attractive forces, it seems reasonable to make this simplifying assumption.

We may then put

$$\tau=\sigma_1\theta_2/\nu \tag{50}$$

and under steady conditions in which $\nu=\mu$ we then have from Eq. (49)

$$\log_{10}(\mu/\theta_2)=27.37-3840/T. \tag{51}$$

Here θ_2 represents the fraction of the available part (θ_1^4) of the first layer which is covered by the adatoms in the second layer. The total number of atoms in the second layer per unit area of true tungsten surface is thus $\sigma_1\theta_1^4\theta_2$.

When μ increases to the value μ_2 corresponding to saturated vapor at the temperature of the filament, θ_2 must rise to unity. Thus by Eq. (51) we have as an equivalent definition of θ_2

$$\theta_2=\mu/\mu_2. \tag{52}$$

In experiments on transients μ or ν must have values which give reasonable time intervals for coating or depleting the surface. With $\mu=10^{11}$ the coating time to $\theta=1$ is one hour and with 10^{15} it is 0.4 second. Let us therefore choose these values of μ and calculate by Eq. (6) for various values of θ_n the corresponding temperatures. These data are given under T in Table V.

With these values of T, putting $\nu=\mu$ we calculate by Eq. (51) the values of θ_2 given in Table V. The values of T in the lowest line are those obtained from Eq. (51) by putting $\theta_2=1$; these are the temperatures at which liquid caesium (polyatomic layers) would condense on the filament.

Examination of these data shows that $\theta_1^4\theta_2$, the number of caesium atoms per unit area in the second layer needed to give an evaporation rate equal to μ is extremely small until θ_1 reaches values of about 0.96. For still higher values of θ_1, θ_2 increases rapidly. When θ_2 becomes comparable with unity, we must take into account the adsorption in the third and higher layers.

Polyatomic layers with nearly saturated vapor

A mathematical theory of the building up of polyatomic adsorbed layers as the vapor approaches saturation has already been given.[23] This theory should now be modified by assuming that adsorption of an atom in the nth layer can occur only on an underlying group of at least 4 atoms in the $(n-1)$st layer. A rough estimate of the number of atoms in each layer may be made by assuming that the number of atoms in the successive layers decreases in the ratio $1:\theta_2^4$. Thus σ, the total number of atoms adsorbed (in all layers) per unit area of the

[23] I. Langmuir, J. Am. Chem. Soc. **60**, 1374 (1918).

TABLE V. *Covering fractions θ_1 and θ_2 for the first and second layers and rates of interchange ρ of atoms between these layers.*

			$\mu=10^{11}$			$\mu=10^{15}$		
θ_n	θ_1	θ_1^4	T°K	θ_2	ρ	T°K	θ_2	ρ
0.5	0.505	0.065	605	9.5×10^{-11}	1.3×10^{17}	789	3.2×10^{-8}	5.6×10^{19}
0.7	.705	.24	516	1.2×10^{-9}	8.4×10^{17}	661	2.8×10^{-7}	2.5×10^{20}
0.9	.905	.67	407	1.2×10^{-7}	1.6×10^{19}	498	2.2×10^{-5}	4.6×10^{21}
0.95	.955	.83	332	1.5×10^{-5}	4.1×10^{20}	391	3.0×10^{-3}	1.7×10^{23}
0.96	.965	.89	306	1.6×10^{-4}	2.1×10^{21}	355	2.8×10^{-2}	8.4×10^{23}
0.97	.975	.91	270	6.9×10^{-3}	2.8×10^{22}	308	—	—
			234	1		310	1	—

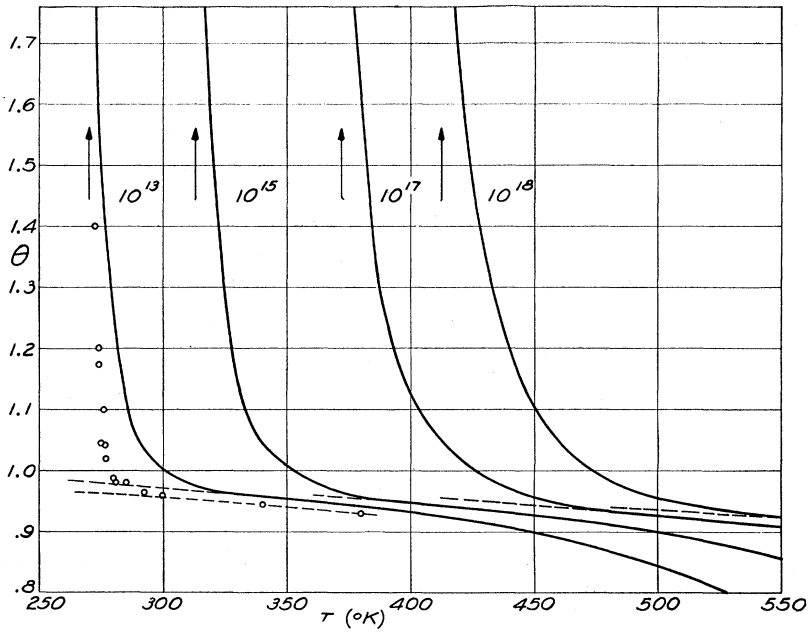

FIG. 27. Formation of a second layer of Cs atoms (calculated by Eqs. (6) and (53)) for different values of μ_a. Arrows give temperature corresponding to saturated Cs vapor. Circles give experimental data obtained at $\mu_a = 10^{13}$.

filament surface, is

$$\theta = \sigma/\sigma_1 = [\theta^1 + \theta_1{}^4\theta_2(1 + \theta_2{}^4 + \theta_2{}^8 + \cdots)]$$

or (53)

$$\theta = [\theta_1 + \theta_1{}^4\theta_2/(1 - \theta_2{}^4)].$$

The rapidly rising portions of the curves in Fig. 10 near $\theta = 0.95$ have been calculated by this equation with values of θ_1 and θ_2 obtained from Eqs. (6) to (10) and (51).

With the bulb containing saturated caesium vapor at a temperature T_s, θ does not exceed unity until the filament temperature T is lowered to within 25° of T_s for $\mu = 10^{11}$ (or 80° for $\mu = 10^{18}$). When $T - T_s$ is 8° (or 24°), θ_2 is 0.3 so that 30 percent of the surface is covered by a second layer of atoms although 2 percent (or 5 percent) of the tungsten surface is still bare (due to repulsive forces in this layer). There are then only enough atoms in the 3rd layer to cover 0.007 of the surface. When $T - T_s$ is 0.6° for $\mu = 10^{11}$ (or 1.9° for $\mu = 10^{18}$) θ_2 is 0.9 so that the covering fractions for the successive layers are roughly 0.98, 0.77, 0.33, 0.14, 0.06, 0.026, etc., the total value of σ/σ_1 being about 2.3.

Experimental test of the formation of polyatomic layers

Fig. 27 shows the building up of a second layer of caesium atoms according to Eq. (53), for various values of μ. The vertical arrows represent the temperatures corresponding to saturated caesium vapor.

It was thought desirable to test for this formation of a second layer. At $\mu_a = 10^{13}$ filament A was maintained, either by passage of small currents or by radiation from filament B, at various temperatures slightly above $T_{\text{sat.}}$ (270°). The temperatures were computed from the measured resistance of the filament.

The adsorbed atom concentration at each temperature was measured by the two filament method. The circles in Fig. 27 give the experimental results. It was found that as indicated by the theory θ increased only slowly until a temperature within 20° of $T_{\text{sat.}}$ was reached. The increase up to this point was closely that given by Eq. (6) for atom evaporation in the first layer.[24] At ~293° a much more rapid rise

[24] This behavior of θ near 1.0 makes it likely that σ_{A1} is more closely 4.9×10^{14} than 4.8×10^{14} as given by the

set in until at 273° a total θ of 1.4 was reached. The direction of the deviation from the theoretical curve shows that atoms evaporate more easily from the 2nd layer of Cs on tungsten than from metallic caesium. Since θ depends on the probability of evaporation of the adsorbed atoms in the 2nd layer, application of the Boltzmann equation serves to indicate the amount by which the heat of evaporation differs from that of liquid Cs.

$$n/n' = \exp(\Delta V e/kT),$$

where n and n' are the theoretical and observed concentrations. Since n/n' is approximately 6 between 275° and 295°, $\Delta V \backsimeq 0.045$ volt. Thus the theory is extraordinarily well confirmed. There is no tendency to form a second layer until near $T_{\text{sat.}}$. Atoms adsorbed in the second layer are not held by forces at all approaching in magnitude those holding Cs directly to tungsten; since ΔV for metallic caesium and Cs adsorbed on tungsten in the first layer is almost 1 volt. The heat of evaporation from the second layer is even less than that from metallic caesium. All this is striking evidence of the true monatomic nature of the first layer of Cs on tungsten.

Mobility and surface diffusion coefficient of adatoms

Let us consider σ adatoms per unit area distributed at random among elementary spaces which are arranged in a square surface lattice, each elementary space being a square of side a so that $a^2 = 1/\sigma_1$. Let τ be the average life of an adatom in a particular space when the 4 adjacent spaces are vacant. The probability per second that an atom in a given space will hop into a given adjacent vacant space is $1/4\tau$. We may take the probability of hopping into an occupied space to be zero. If we may assume that the atoms exert no appreciable forces on one another (except that needed to keep 2 out of a single space), τ may be taken to be independent of σ.

The flux φ of atoms per cm of length across a line midway between two adjacent rows (A and B) of elementary spaces (perpendicular to X axis) is

$$\varphi_{AB} = (a\sigma_A/4\tau)(1-\sigma_B/\sigma_1) \quad \text{from } A \text{ to } B$$
and (54)
$$\varphi_{BA} = (a\sigma_B/4\tau)(1-\sigma_A/\sigma_1) \quad \text{from } B \text{ to } A.$$

The net flux or drift flux φ_D is thus

$$\varphi_D = (a/4\tau)(\sigma_A - \sigma_B) = (a^2/4\tau)d\sigma/dx. \quad (55)$$

The surface diffusion coefficient D may be defined by equating φ_D to $D\, d\sigma/dx$ and thus we find for all values of θ from 0 to 1

$$D = a^2/4\tau = 1/4\sigma_1\tau. \quad (56)$$

In case we have to deal with a hexagonal surface lattice in which atoms may hop to any one of six adjacent spaces, this equation needs to be modified merely by replacing the 4 in the denominator by 3. For tungsten surfaces which have been highly heated, the atoms are arranged in a surface lattice in which the elementary rectangle of dimensions 3.15×4.46A has one atom at each corner and one atom in the center. Each surface atom has thus 4 near neighbors and therefore Eq. (56) should be applicable.

This equation has been derived on the assumption that the time τ during which an atom remains in an elementary space is large compared to a/v, the time required for the passage of an atom from one space to the next.

When the time of transit a/v is not negligible, Eq. (56) needs to be modified merely by adding a/v to τ so that

$$D = a^2/4(\tau + a/v_2), \quad (57)$$

where v_2 the average velocity parallel to the plane of the surface (2-dimensional velocity) is given in cm sec.$^{-1}$ by

$$v_2 = (\pi kT/2m)^{\frac{1}{2}} = 11{,}428(T/M)^{\frac{1}{2}}, \quad (58)$$

M being the molecular or atomic weight.

If τ is negligible compared to a/v_2, this reduces to

$$D = (1/4)av_2. \quad (59)$$

In the elementary kinetic theory of gases it is shown[25] that the coefficient of self-diffusion of a gas is $D = (1/3)\lambda_3 v_3$ where v_3 is the average

previous less detailed experiments of Section V, introducing a possible error of about 2 percent in the calculations of θ.

[25] See for example *Dynamical Theory of Gases*, J. H. Jeans, p. 326, Cambridge, 2nd Edition.

(3-dimensional) molecular velocity and λ_3 is the 3-dimensional free path. A similar calculation for the 2-dimensional case of surface diffusion leads to

$$D=(1/2)\lambda_2 v_2, \tag{60}$$

where λ_2 is now the length of the projection of the free path on the plane of the surface. If we identify λ_2 with a, this equation is the same as Eq. (59) except for the numerical factor. This difference is due to the fact that in deriving Eq. (60) it was assumed that all directions of motion in the plane are equally probable, while for Eq. (59) the motions were taken to be parallel to the two axes of the square lattice.

Measurements of the surface diffusion coefficient D_1 for Cs adatoms on tungsten for an average value of θ of about 0.03 have given,[15] for the temperature range from 650 to 812°K,

$$\log_{10} D_1=-0.70-3060/T. \tag{61}$$

Since the number of tungsten atoms per cm^2 on a tungsten surface is 1.425×10^{15} we must take this to be the number of elementary spaces and thus get

$$a_1=2.64\times10^{-8}\text{ cm}. \tag{62}$$

Using this value of a_1 and the value of v_2 from Eq. (58) we calculate τ_1 at various temperatures in the range from 650 to 812° and find that they are represented by

$$\log_{10}\tau_1=-15.09+3082/T. \tag{63}$$

Values of τ_1 and D_1 (for Cs atoms in the 1st layer) are given for several temperatures in the 3rd and 2nd columns of Table VI.

TABLE VI. *Surface diffusion coefficients for Cs adatoms in 1st and 2nd layers.* τ_1 and τ_2 are the "lives" in elementary spaces in 1st and 2nd layers as given by Eqs. (63) and (64); τ is the "evaporation life" in 2nd layer given by Eq. (49).

T	D_1(cm^2 sec.$^{-1}$)	τ_1(sec.)	τ_2	a_2/v_2	D_2	τ
			$\times10^{-14}$	$\times10^{-14}$		
300	1.2×10^{-11}	1.5×10^{-5}	175.	31.	0.00034	0.95
400	4.3×10^{-9}	4.1×10^{-8}	26.	27.	.00134	5.9×10^{-4}
500	1.5×10^{-7}	1.2×10^{-9}	8.1	24.	.0022	7.2×10^{-6}
600	1.6×10^{-6}	1.1×10^{-10}	3.8	22.	.0027	3.8×10^{-7}
700	$8.\times10^{-6}$	2.1×10^{-11}	2.2	20.	.0032	4.6×10^{-8}

The mobility of adatoms in the 2nd layer must be much greater than that in the 1st layer since the atoms in the 2nd layer are held by much weaker forces. For low values of θ_1 at which D_1 was measured, the heat of evaporation of atoms from the 1st layer is 2.83 volts. The potential barrier corresponding to the coefficient of $1/T$ in Eq. (63), 3082, is, as we have seen, 0.61 volt which is 21.5 percent of the heat of evaporation. The potential barrier separating the elementary spaces for the 2nd layer must be much less than 0.61 volt which is 78 percent of the heat of evaporation (0.79 volt) from the 2nd layer. It seems reasonable to assume that the barrier in this case also is approximately 21.5 percent of the heat of evaporation. This would give 0.17 volt. The Cs atoms in the 1st layer, however, because of their larger size compared to W atoms, constitute a rougher support for the atoms in the 2nd layer than is provided for the 1st layer of atoms by the underlying tungsten surface. Thus we may adopt the rough value 0.2 volt as most probable value for the barrier in the 2nd layer. This corresponds to a coefficient 1000 for $1/T$. This gives for the life τ_2 of an adatom in an elementary space of the 2nd layer

$$\log_{10}\tau_2=-15.09+1000/T. \tag{64}$$

We have taken the term -15.09 to be the same as in Eq. (63), since for evaporation[26] and for diffusion[27] this term remains nearly constant even for different substances.

Thus a general equation for the evaporation life τ was found[26] to be

$$\tau=4.7\times10^{-27}M^{\frac{1}{2}}\sigma_1 T^{-1}\epsilon^{b/T}. \tag{65}$$

Because of the similarity of the processes of evaporation and of mobility, by which atoms hop from one position to another, we may expect this equation to be at least roughly applicable to surface diffusion. Putting $M=133$, $\sigma_1=3.56\times10^{14}$ and $T=500$ (the mean temperature) we find from Eq. (65)

$$\log_{10}\tau=-13.4+0.43b/T. \tag{66}$$

The values of τ_2 calculated from this equation by putting $0.43b=1000$ are of roughly the same

[26] Reference 2. See particularly Eq. (37) on page 2806.
[27] S. Dushman and I. Langmuir, Phys. Rev. **20**, 113 (1922).

magnitude as those by Eq. (64). A change of about 10 percent in the assumed value of the coefficient of $1/T$ would bring the two equations into agreement at a given temperature.

The values of τ_2 calculated from Eq. (64) are given in the 4th column of Table VI, and D_2 calculated from these by Eq. (57) taking

$$a_2 = 5.3 \times 10^{-8} \tag{67}$$

is given in the 6th column while the time of transit a_2/v_2 is given in the 5th column.

The last column of Table VI gives the evaporation life of adatoms in the 2nd layer as calculated from Eq. (49). Comparing τ with τ_2 and a_2/v_2 we see that at $T=300$ each adatom in the 2nd layer moves through about 10^{12} elementary spaces before evaporating and even at 700° it moves through 10^5 spaces during its life. This fact affords a simple explanation of the high values of α.

Surface random flux

A very useful concept[28] in the study of electric discharges in gases is that of random current density I_e. If n is the number of electrons per unit volume in a uniform plasma and v is their average velocity, then across any imaginary plane there is a current density $I_e=(1/4)nve$ of electrons which pass across the plane from one side to the other and an equal current of electrons passing back in the opposite direction.

Similarly for the motions of adatoms on any surface in a steady state we may define the *random flux density* φ as the number of atoms per unit length which cross any imaginary line in the surface from one side to the other (while an equal flux passes in the opposite direction).

If the adatoms move in random directions parallel to the plane of the surface with the average velocity v, then one-half the atoms on one side of the line are approaching the line with an average velocity $(2/\pi)v$. Thus we find

$$\varphi = (1/\pi)\sigma v = (\sigma_1/\pi)\theta v. \tag{68}$$

If the adatoms, instead of moving with uniform velocity, hop from space to space as postulated in the derivation of Eqs. (54), (55) and (57), we obtain

$$\varphi = a\sigma_1\theta(1-\theta)/4(\tau + a/v_2) = (\sigma_1 D/a)\theta(1-\theta). \tag{69}$$

Rate of interchange of atoms between the first and second adsorbed layers

Consider that the first layer in a square surface lattice is nearly completely filled by adatoms as indicated in Fig. 28, so that the $\sigma_1(1-\theta_1)$ vacant

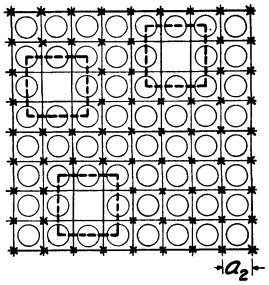

FIG. 28. First layer in a square surface lattice nearly completely filled by adatoms, denoted by circles. Available spaces in the second layer are indicated by crosses.

spaces per unit area are separated from one another. The available elementary spaces in the second layer are indicated in the figure by crosses. Each vacant space in the first layer causes a decrease of four in the number of available spaces in the second layer; this number per unit of filament surface is therefore $\sigma_1[1-4(1-\theta_1)]$, which for values of θ_1 close to unity agrees with $\sigma_1\theta_1^4$ as deduced previously.

Any adatom in the second layer which migrates across the dotted line in Fig. 28, which has a perimeter $8a_2$, evidently falls into the vacant space in the first layer. Thus the rate ρ at which atoms pass from the second to the first layer, expressed in atoms cm^{-2} $sec.^{-1}$, is

$$\rho = 8a_2\varphi_2\sigma_1(1-\theta_1). \tag{70}$$

Under equilibrium conditions this must be balanced by the passage of an equal number of atoms from the 1st to the 2nd layers. Thus ρ may be termed the *rate* of *interchange* between the 2 layers. If this rate is very high compared to the rates of evaporation ν or condensation μ from or to the surface, the relative numbers of adatoms in the two layers $\sigma_1\theta_1$ and $\sigma_1\theta_2\theta_1^4$ will be the same whether or not the adsorbed films are in equilibrium with the vapor phase. There-

[28] I. Langmuir and H. Mott-Smith, G. E. Rev. **27**, 449 (1924); I. Langmuir and K. T. Compton, Rev. Mod. Phys. **3**, 221 (1931).

fore the conditions for which the surface phase postulate will be fulfilled are $\rho/\nu \gg 1$, and $\rho/\mu \gg 1$.

In deriving Eq. (70) we considered the rate at which atoms in the 2nd layer move to and drop into holes in the 1st layer. It is, however, possible, because of the mobility in the 1st layer, for holes in the 1st layer to move to atoms in the 2nd layer. Considerations like those used in deriving Eq. (69) lead to the conclusion that the diffusion coefficient for *holes* is the same as for *atoms* and that the surface flux of holes as well as that of atoms is given by the last member of Eq. (69). Taking Eq. (70), after eliminating φ_2 by Eq. (69),

$$\rho = 8\sigma_1^2(D_2+\theta_1 D_1)(1-\theta_1)\theta_2(1-\theta_2). \quad (71)$$

The values of ρ given in Table V were obtained by this equation, with the data for D_2 given by Table VI. They are large compared with μ or ν and therefore the surface phase postulate applies.